NeuroImage: Clinical 38 (2023) 103383

Contents lists available at ScienceDirect

NeuroImage: Clinical

journal homepage: www.elsevier.com/locate/ynicl

The association between white matter hyperintensities and amyloid and tau deposition

Sierra L. Alban [a], Kirsten M. Lynch [a], John M. Ringman [b,c], Arthur W. Toga [a,b], Helena C. Chui [b,c], Farshid Sepehrband [a], Jeiran Choupan [a,d], For the Alzheimer's Disease Neuroimaging Initiative [*]

[a] Laboratory of NeuroImaging, USC Stevens Neuroimaging and Informatics Institute, Keck School of Medicine, University of Southern California, Los Angeles, CA, USA
[b] Alzheimer's Disease Research Center, Keck School of Medicine, University of Southern California, Los Angeles, CA, USA
[c] Department of Neurology, Keck School of Medicine, University of Southern California, Los Angeles, CA, USA
[d] NeuroScope Inc., Scarsdale, NY, USA

A B S T R A C T

White matter hyperintensities (WMHs) frequently occur in Alzheimer's Disease (AD) and have a contribution from ischemia, though their relationship with β-amyloid and cardiovascular risk factors (CVRFs) is not completely understood. We used AT classification to categorize individuals based on their β-amyloid and tau pathologies, then assessed the effects of β-amyloid and tau on WMH volume and number. We then determined regions in which β-amyloid and WMH accumulation were related. Last, we analyzed the effects of various CVRFs on WMHs. As secondary analyses, we observed effects of age and sex differences, atrophy, cognitive scores, and APOE genotype. PET, MRI, FLAIR, demographic, and cardiovascular health data was collected from the Alzheimer's Disease Neuroimaging Initiative (ADNI-3) (N = 287, 48 % male). Participants were categorized as A + and T + if their Florbetapir SUVR and Flortaucipir SUVR were above 0.79 and 1.25, respectively. WMHs were mapped on MRI using a deep convolutional neural network (Sepehrband et al., 2020). CVRF scores were based on history of hypertension, systolic and diastolic blood pressure, pulse rate, respiration rate, BMI, and a cumulative score with 6 being the maximum score. Regression models and Pearson correlations were used to test associations and correlations between variables, respectively, with age, sex, years of education, and scanner manufacturer as covariates of no interest. WMH volume percent was significantly associated with global β-amyloid ($r = 0.28$, $p < 0.001$), but not tau ($r = 0.05$, $p = 0.25$). WMH volume percent was higher in individuals with either A + or T + pathology compared to controls, particularly within in the A+/T + group ($p = 0.007$, Cohen's $d = 0.4$, $t = -2.5$). Individual CVRFs nor cumulative CVRF scores were associated with increased WMH volume. Finally, the regions where β-amyloid and WMH count were most positively associated were the middle temporal region in the right hemisphere ($r = 0.18$, $p = 0.002$) and the fusiform region in the left hemisphere ($r = 0.017$, $p = 0.005$). β-amyloid and WMH have a clear association, though the mechanism facilitating this association is still not fully understood. The associations found between β-amyloid and WMH burden emphasizes the relationship between β-amyloid and vascular lesion formation while factors like CVRFs, age, and sex affect AD development through various mechanisms. These findings highlight potential causes and mechanisms of AD as targets for future preventions and treatments. Going forward, a larger emphasis may be placed on β-amyloid's vascular effects and the implications of impaired brain clearance in AD.

1. Introduction

Alzheimer's Disease (AD) is traditionally characterized by the presence of β-amyloid plaques and neurofibrillary tangles of tau proteins in the brain (Villemagne et al., 2018). Other pathophysiological changes have been associated with AD, particularly those related to vascular pathology (Kalaria et al., 2012). For example, several studies have established a relationship between higher white matter lesion volume and cognitive decline (Au et al., 2006; Burton et al., 2004; Gunning-Dixon and Raz, 2003).

White Matter Hyperintensities (WMHs) are lesions occurring in the brain's white matter best detected as areas of hyperintense signal appearing in T2- weighted or FLAIR sequences on MRI (Lin et al., 2017). These WMHs may ultimately be caused by cardiovascular risk factors (CVRFs), such as hypertension (both systolic and diastolic), and body mass index that may affect cerebral blood flow (Kisler et al., 2017; Murray et al., 2005; Gottesman et al., 2010; Breteler et al., 1994; Liao et al., 1997; Liao et al., 1996). WMHs have also been linked to cerebral amyloid angiopathy (CAA), the deposition of amyloid in the walls of small cerebral blood vessels (Holland et al., 2008; Gurol et al., 2006; Chen et al., 2006). Alternate vascular events such as non-CAA cerebral small vessel disease, stroke, and carotid atherosclerosis, among others,

[*] Data used in preparation of this article were obtained from the Alzheimer's Disease Neuroimaging Initiative (ADNI) database (adni.loni.usc.edu). As such, the investigators within the ADNI contributed to the design and implementation of ADNI and/or provided data but did not participate in analysis or writing of this report. The ADNI was launched in 2003 as a public-private partnership, led by Principal Investigator Michael W. Weiner, MD. A complete listing of ADNI investigators can be found at: http://adni.loni.usc.edu/wp-content/uploads/how_to_apply/ADNI_Acknowledgement_List.pdf

https://doi.org/10.1016/j.nicl.2023.103383
Received 12 October 2022; Received in revised form 9 February 2023; Accepted 16 March 2023
Available online 20 March 2023
2213-1582/© 2023 The Author(s). Published by Elsevier Inc. This is an open access article under the CC BY-NC-ND license (http://creativecommons.org/licenses/by-nc-nd/4.0/).

are hypothesized to contribute to WMH burden (Pico et al., 2002; DeCarli et al., 1999) However, white matter lesions may also arise in association with normal aging (Duanping et al., 1996). Many of these studies investigating vascular risk and AD have found that earlier onset and co-occurrence of CVRFs increases the likelihood of accelerated cognitive decline later in life (Debette et al., 2011; Maillard et al., 2015). Ultimately the interactions between AD pathophysiology and various risk factors are not entirely clear.

The relationship between WMH and AD pathology is incompletely characterized. There is a variety of data relating the existence of β-amyloid and tau with increasing WMH volume. Literature addressing the ability of these biomarkers to predict WMHs demonstrate only that β-amyloid is correlated with WMH burden (Graff-Radford et al., 2019; Grimmer et al., 2012). There is assorted research highlighting a relationship between vascular risk factors and various AD pathologies, despite the common understanding that vascular health plays a significant role in the development of AD (Rabin et al., 2019). Many studies in this field have contradicting results, some associating CVRFs with only β-amyloid, others finding additional associations with tau, or finding no AD neuropathological association whatsoever (Gottesman et al., 2017; Vemuri et al., 2017; Rabin et al., 2019; Conner et al., 2019, Lane et al., 2020). Cerebrospinal fluid measures of β-amyloid and tau are often used to investigate associations with WMHs and CVRFs, though there is growing interest in the use of positron emission tomography (PET) since it is less invasive and more regionally specific (Palmqvist et al., 2015; Walsh et al., 2020; Tosto et al., 2015; Dadar et al., 2020; Morrison et al., 2022). As interest in PET biomarkers increases, more studies are needed to assess its diagnostic accuracy compared to CSF methodology. Lastly, recent research has highlighted a potential regional component of β-amyloid and WMH accumulation in the brain influencing AD symptom progression, though few studies have evaluated the regional colocalization of WMHs with β-amyloid PET markers in disease manifestation (Roseborough et al., 2017; Weaver et al., 2019; Grimmer et al., 2012; Tan et al., 2022). It is important to properly gauge the role of AD pathology and CVRFs in vascular lesion formation to improve our understanding of AD risk.

Particular biomarkers, such as Florbetapir and Flotaucipir PET measures of β-amyloid and neurofibrillary tangles, respectively, have been utilized to identify the presence of AD pathology. The National Institute of Aging and the Alzheimer's Association (NIA-AA) recently updated diagnostic categories for AD using this biomarker AT(N) classification system, specifically for research applications (Jack et al., 2018). It accounts for β-amyloid (A), tau (T), and neurodegeneration (N), with '+' denoting the presence and '–' denoting the absence of each biomarker (Jack et al., 2016). Variations in the AT(N) classification categorize individuals based on pathologic change. The goal of this framework is to understand disease progression and pathogenesis more accurately. The present study specifically utilizes this framework to observe risk factor and biomarker differences across the pathological groups.

Studies of sex differences for AD risk factors have found differential results regarding CVRFs, β-amyloid, tau, and WMH volume. Specifically, risk factors for WMHs affect men and women differently, with women seemingly more susceptible to WMH accumulation (Koran et al., 2017). Overall, more research is needed to better understand the differential effects of risk factors across sexes and how they manifest into disease. Homozygous APOE-*ε4* genotype is the genetic marker that significantly increases one's risk for AD (Corder et al., 1993). APOE-*ε4* has also been shown to be associated with other hallmarks of AD, including WMHs (Rojas et al., 2018). Ultimately, the mechanism by which β-amyloid is related to WMH volume and count may be different for those with homozygous APOE-*ε4* genotypes. Furthermore, decreased hippocampal volume as a measure of atrophy is a commonly known AD pathology and is often used to help determine disease stage (de Leeuw et al., 2004; Convit et al., 1997; Schuff et al., 2009) For these reasons, inclusion of age, sex, APOE-ε4, and atrophy measures in the evaluation of AD risk is beneficial.

In this study, we initially analyzed the relationship between AD pathology and both WMH volume and count, across pathological groups and with varying β-amyloid and tau burdens. We then went on to identify factors that may contribute to the observed relationship between WMH burden and AD pathology, including CVRF, age, and sex. Secondarily, the effects of homozygous APOE-*ε4* genotype, atrophy, and cognitive scores on β-amyloid and WMH volume were also assessed. Finally, we explored a cortical region localized analysis to observe associations between β-amyloid and WMH amount across the brain.

2. Methods

2.1. Participants

All data used in the present study was obtained from the Alzheimer's Disease Neuroimging Initiative (ADNI) database (https://adni.loni.usc.edu). ADNI was launched in 2003 by the National Institute on Aging, the National Institute of Biomedical Imaging and Bioengineering, the Food and Drug Administration, private pharmaceutical companies, and non-profit organizations. The goal of ADNI is to identify and track Alzheimer's Disease in its early stages through various biomarkers.

ADNI includes clinical data for subjects such as demographic information, vital signs, cognitive assessments, and comprehensive medical history, among other variables not involved in this study. Across all 286 participants, 199 were scanned with Siemen's scanners, 71 with GE scanners, and 16 with Philips scanners.

Cognitive assessments were conducted following standardized protocols consistent with published procedures. The Montreal Cognitive Assessment (MoCA) is a brief cognitive assessment that specifically tests for individuals with mild cognitive impairments (MCI). The Mini Mental State Examination (MMSE), like the MoCA, is a brief screening for AD that evaluates orientation, memory, attention, concentration, naming, repetition, comprehension, ability to create a sentence, and ability to copy two overlapping pentagons. Global Clinical Dementia Rating (CDR) describes five degrees or impairment by testing six categories of cognitive functioning: memory, orientation, judgement and problem solving, community affairs, home and hobbies, and personal care.

Cognitively normal (CN) participants are defined as possibly having subjective memory complaints beyond what is expected for the age, normal memory function with respect to education level in the Logical Memory II subscale, an MMSE score between 24 and 30, a CDR of 0, absence of significant impairment in cognitive functions or daily activities, and stability of permitted medications for 4 weeks (antidepressants without significant anticholinergic side effects, estrogen replacement therapy, gingko biloba, psychoactive medication washout for at least 4 weeks prior to screening).

Mild cognitively impaired (MCI) participants must express subjective memory concerns, have abnormal memory function and scoring below education level in the Logical Memory II subscale, have an MMSE between 24 and 40, have a CDR of 0.5, have general cognition and functional performance preserved such that there is no AD diagnosis, and similar medication requirements as CN participants with the addition of cholinesterase inhibitors and memantines allowed.

Alzheimer's Disease (AD) participants must express subjective memory concern, have abnormal memory function by education level, an MMSE between 20 and 24, a CDR of 0.5 or 1,0, criteria for probable AD by the National Institute of Neurological and Communicative Disorders and Stroke and the Alzheimer's Disease and Related Disorders Association (NINCDS-ADRDA), and the same medication guidelines as MCI participants.

The distributions of participants were 138 in the A-/T- group (age: 75.1 ± 7.6), 82 in the A+/T- group (age: 76.4 ± 7.7), 12 in the A-/T + group (age: 78.1 ± 8.2), and 54 in the A+/T + group (age: 76.1 ± 8.1). According to the NIA-AA research framework, A-/T- participants are considered normal, A-/T + is considered non-AD pathologic change,

A+/T- is considered AD pathologic change, and A+/T + is considered AD (Jack et al. 2018). See Table 1 for more detail on the participants. Demographic information including age, sex, and years of education, and scanner manufacturer was used as covariates in all statistical analyses.

2.2. Cardiovascular Risk Factors

Vascular risk factors including history of hypertension, measurements of systolic and diastolic blood pressure, respiration and pulse rate, and body mass index (BMI) were assessed by medical history and measured in a physical examination by a medical professional. History of hypertension was identified by self-report. Both systolic and diastolic blood pressure were identified as risk factors if elevated above the Centers for Disease Control and Prevention guidelines (greater than 130 mmHg or 80mHg respectively). Respiration rate was considered a risk factor if outside the normal range of 12–25 breaths per minute. Similarly, pulse rate was considered a risk factor if not within the healthy range of 60–80 beats per minute. Both pulse rate and respiration rate guidelines are from the Cleveland Clinic (2019). BMI was considered a risk factor if greater than 25, as suggested by the Centers for Disease Control and Prevention. Total CVRFs were calculated as a sum of each individual risk factor's presence, with a score of 6 being the highest possible. This cumulative score is an adaptation of other measurements of cardiovascular disease risk, such as the Framingham risk score, but using six possible measures of cardiovascular disease (Wilson et al., 1998, Kannel et al., 1976).

Table 1
Abbreviations: N, number of participants. BP, blood pressure. BMI, body mass index. MOCA, Montreal Cognitive Assessment. MMSE, Mini Mental State Exam Total Score. CDR, Clinical Dementia Rating. CN, Cognitively Normal. MCI, Mild Cognitive Impairment. AD, Alzheimer's disease. APOE4 Homozygous, Frequency of APOE4 homozygous subjects. APOE4 Presence, Presence of 1 or more APOE4 alleles WMH, White Matter Hyperintensity. SUVR, standard uptake value ratio.

Measures	A-/T-	A-/T+	A+/T-	A+/T+	Statistical p-value
N	138	12	82	54	
Female, N(%)	71(51.4 %)	4(33.3 %)	42(51.2 %)	32(59.3 %)	0.415
Age (y)	73.7 ± 7.19	78.1 ± 8.19	76.4 ± 7.69	76.1 ± 8.07	0.002
Education(y)	16.6 ± 2.63	18.4 ± 1.83	16.6 ± 2.47	15.6 ± 2.34	0.028
Hypertension, N (%)	24(39.3 %)	1(33.3 %)	12(38.7 %)	12(50 %)	0.799
Systolic BP	133.6 ± 17	130 ± 14.9	127.9 ± 18.7	134.6 ± 16.5	0.444
Diastolic BP	74.2 ± 8.55	69.8 ± 6.9	71.1 ± 8.81	75 ± 7.88	0.444
Respiration Rate	15.9 ± 2.57	16.4 ± 2.1	15.99 ± 3.3	15.5 ± 2.21	0.190
Pulse Rate	63.5 ± 10.3	60 ± 10.1	64.8 ± 11.5	64.6 ± 9.0	0.532
BMI	28.1 ± 5.32	26.2 ± 5.18	26.4 ± 4.47	25.1 ± 3.42	2.2e-8
Total CVRF score	3.0 (1.5)	2.0 (0.5)	2.0 (2.0)	3.0 (1.5)	0.525
MOCA	25.2 ± 2.89	24.0 ± 2.52	24.1 ± 3.91	19.9 ± 9.90	2.54e-10
MMSE	29.0 ± 1.26	28.3 ± 2.57	28.4 ± 2.24	25.0 ± 13.44	7.97e-9
Global CDR	0.11 ± 0.21	0.25 ± 0.40	0.15 ± 0.27	0.57 ± 1.06	9.21e-8
CN	107 (77.5 %)	6(50 %)	58(70.7 %)	15(27.8 %)	1.01e-9
MCI	30(21.7 %)	6(50 %)	18(22.0 %)	19(35.2 %)	0.046
AD	1(0.72 %)	0 (0 %)	6(7.32 %)	20(37.0 %)	2.15e-13
APOE4 Homozygous	2 (1.45 %)	0 (0 %)	6 (7.3 %)	8 (14.8 %)	0.005
APOE4 Presence	27 (20 %)	2 (16.7 %)	27 (32.9 %)	26 (48.1 %)	0.6e-4
WMH Volume %	0.33 ± 0.52	0.84 ± 0.90	0.72 ± 1.14	0.55 ± 0.61	0.002
WMH Count	14.6 ± 11.3	18.1 ± 11.1	18.2 ± 11.6	18.7 ± 8.8	0.27e-4
β-amyloid SUVR	0.73 ± 0.03	0.73 ± 0.05	0.91 ± 0.10	1.02 ± 0.12	6.54e-84
Tau SUVR	1.09 ± 0.08	1.32 ± 0.11	1.11 ± 0.09	1.27 ± 0.31	4.21e-26

2.3. Data Collection

Magnetic resonance imaging (MRI), amyloid and tau PET along with demographic data of participants of Alzheimer's disease neuroimaging initiative (ADNI-3) were downloaded from LONI imaging data archive (https://ida.loni.usc.edu) as explained in Weiner et al., 2017. ADNI-3 MRI data was acquired using standardized protocols on Philips, Siemens, and GE 3 T scanners at 63 study sites across North America. 3D T1-weighted images were acquired with an MPRAGE sequence (Philips and Siemens scanners) and FSPGR sequence (GE scanner) with the following parameters. MPRAGE: TR = 2300 ms echo time, TE = 2.98 ms, voxel resolution: 1 mm^3, FOV = 240x256mm^2, matrix = 240x256 (with variable slice number), TI = 900 ms, flip angle = 9. FSPGR (with sagittal slices): TR = 7.3 ms, TE = 3.01 ms, FOV = 256x256mm^2, matrix = 256x256mm (with variable slice number), TI = 1650 ms, flip angle = 120. 3D FLAIR images were acquired with the following acquisition parameters: TR/TE: 4800/119, voxel resolution = 1x1x1.2 mm^3, FOV = 256x256mm^2, matrix = 256x256 (variable slice number), TI = 1650 ms, flip angle = 120. PET imaging protocols included Flobetapir (Amyvid) and Flortaucipir (AV-1451). Florbetapir imaging lasted 20 min, with four 5-minute frames, and acquisition occurred 50–70 min post-injection. Flortaucipir imaging acquisition occurred 30–60 min post-injection and lasted 30 min, using six 5-minute frames. Data used for this study was from the subset of ADNI-3 participants who had all the T1-wighted, 3D FLAIR, Amyloid and Tau PET modalities available.

2.4. Quality control processing

All FLAIR and T1w MRI images were quality controlled for misalignment and post-processing failure, blind to clinical and neuroimaging measures. Of the 408 ADNI3 participants with 3D FLAIR, T1W, and PET data, 122 were excluded due to failing this quality control. This led to a total of 286 participants (137 male, 48 %) that were further separated into groups based on their amyloid and tau pathologies.

2.5. MRI Preprocessing

Data processing was completed using the Laboratory of Neuro Imaging Pipeline (https://pipeline.loni.usc.edu/) and the FreeSurfer (v5.3.0) software package was used for T1w preprocessing and parcellation (Fischl, 2012). The Desijan-Killany atlas was used for brain volume and white matter masks, then the *recon-all* module of FreeSurfer was used to complete the parcellation. This atlas parcellates the cortex into 68 regions as well as the underlying white matter. To be sure of white matter coverage, the centrum semi-ovale of the white matter region from the Freesurfer output was used. According to FreeSurfer, the centrum semi-ovale is made up of 'Unsegmented white matter', 5001 and 5002 from Desikan-Killiany-Tourville adult cortical parcellation atlas, which is near the ventricles and includes part of the ventricles as well as the internal and external capsules in the white matter mask. For this reason, we used the centrum semi-ovale mask shown in **Supplemental** Figure S1 and **Supplemental** **Table S5** which excludes the internal/external capsules and the ventricles. Non-uniform intensity normalization, intensity normalization, skull stripping motion correction, and Talairach transform computation is all included in the *recon-all*

preprocessing procedure (Dale et al., 1999; Desikan et al., 2006; Fischl et al., 1999, 2002, 2004; Fischl and Dale, 2000; Reuter et al., 2010, 2012; Reuter and Fischl, 2011; Ségonne et al., 2004; Segonne et al., 2007; Sled et al., 1998; Waters et al., 2019).The N41TK module from Advanced Normalization Tools (ANTs) (Avants et al., 2009) was used to correct non-uniform field inhomogeneity in FLAIR images (Tustison et al., 2010). Then, they were co-registered with T1w images with the *antsIntermodalityIntrasubject* module from ANTs.

2.6. WMH Mapping

A previously reported multi-step image processing approach was used as described in Sepehrband et al., 2021. WMH segmentation was trained on 685 patients on ADNI (including data used in this study). F1 Score (also known as Dice similarity index) was used to assess the segmentation accuracy on 10 % of the data which was manually analyzed by an expert reader. The segmentation resulted in F1 Score of 95 ± 3 % (M ± SD). WMHs are hyperintense in FLAIR images and hypointense in T1w images, a signature which was used to improve the segmentation accuracy compared to a technique solely based on FLAIR. WMH are falsely identified as enlarged PVS due to their similar isointense or hypointense appearance (although not as hypointense as CSF) on T1-weighted sequences (Wardlaw et al., 2013). We mapped WMH from FLAIR using conventional algorithmic approaches (Wetter et al., 2016). Then we estimated the likelihood of a voxel belonging to perivascular space (PVS) in T1w image, which also appears hypointense in T1w images (Sepehrband et al., 2019), using Frangi filtering which computes the vesselness measure for each voxel from eigenvectors of the Hessian matrix of the T1w image (Frangi et al., 1998). The FLAIR image of each subject was then corrected for non-uniform field inhomogeneity using N4ITK module (Tustison et al., 2010) of Advanced Normalization Tools (ANTs) (Avants et al., 2009). The FLAIR image was then co-registered to T1w image using ANTs software. For each voxel with high vesselness likelihood we estimated the percentile of the FLAIR intensity in a given geodesic distance across the voxels within the white matter. Voxels with high FLAIR intensity were added to a temporary WMH mask, and those with low 10 percentile were segmented as PVS. Then, a convolutional neural network was trained on the co-registered multi-modal (T1w and FLAIR) WMH masks to create an automated WMH segmentation. Training was performed on ADNI-3 subjects using network architecture and configuration from Kamnitsas et al., 2017.

Morphological analysis was used to count the WMH. Connected components were considered as individual WMH. The measurement used connectivity of 8 for two dimensions and 26 for three dimensions.

2.7. Amyloid and Tau PET processing

To categorize individuals into Aβ +/-, amyloid PET data was used and analyzed according to UC Berkeley PET methodology (Baker et al., 2017; Landau et al., 2014; Landau et al., 2015; Schöll et al., 2016). Florbetapir (^{18}F-AV-45, Avid) was used to image uptake of amyloid, using six 5-minute frames. These frames were co-registered to frame 1 using NeuroStat "mcoreg" module with rigid-body translation and six degrees of freedom. The frames were averaged and reoriented into a 160x160x96 grid with 1.5 mm voxels so that the anterior-posterior axis of the subject was aligned with the anterior-posterior commissure line.

Using the mutual information algorithm in SPM5 with default setting, the PET images were co-registered on T1w MRI to align parcellation regions. Standard Uptake Value ratio (SUVR) was used for quantitative measurements. Mean tracer uptakes were calculated in frontal, lateral parietal, lateral temporal, and anterior/posterior cingulate cortices. The cerebellar mean was calculated and used for reference. To calculate the entire cortical SUVR, the mean tracer uptake in each cortical region was averaged and divided by the cerebellum reference mean. Flortaucipir (^{18}F-AV-1451) was used for Tau PET to assess accumulation of tau in several regions of the temporal lobe (defined by Jack et al., 2018: entorhinal cortex, amygdala, parahippocampal, fusiform, inferior temporal, and middle temporal regions of interest). Increased tau SUVR in these medial temporal regions are associated with Braak Stage I and II (Lowe et al., 2018, Braak and Braak, 1991). Additionally, the amygdala, parahippocampal, entorhinal, fusiform, inferior temporal, and middle temporal regions are the first to indicate ligand uptake in the aged clinically normal population. While uptake in the basal or lateral temporal lobe are more associated with hallmarks of AD (Jack et al., 2016, Johnson et al., 2016). Tau PET SUVR was processed similar to the amyloid PET above, and Tau SUVR values were normalized utilizing the intensity of cerebellar gray matter. The cutoffs used to categorize A + and T + were any values above 0.79 and 1.25 respectively, and any below these fell into A- and T- categories (Jack et al. 2016).

2.8. Statistical analysis

A regression model was used to assess the association between WMH and accumulation of amyloid, in which Aβ SUVR was used as dependent variable, and percentage of white matter occupied by WMH as independent variable, controlling for age, sex, years of education, and scanner manufacturer. An ordinary least square fitting model was used to fit the linear regression to the data using StatsModels Python library. A similar regression analysis was used with Tau SUVR as the dependent variable to determine the association between Tau and WMH.

Cohen's *d* statistics are useful in indicating the magnitude of difference between groups for a specific variable, with a larger statistic indicating a greater difference between means. Unpaired Cohen's *d* effect size was used to assess the WMH volume mean differences across groups with different pathology status: A-/T-, A-/T+, A+/T-, A+/T +. The Cohen's *d* (effect size) and two-sided *p*-value of the group differences were measured using estimation statistics of Mann-Whitney test from DaBest toolbox (Ho et al., 2019). The p-value(s) of$<$0.05 reported are the likelihood(s) of observing the effect size(s) if the null hypothesis of zero difference is true. We also used the SciPy Python library to assess whether WMH volume and WMH count were normally distributed across pathological groups.

To assess the influence of CVRFs on WMH volume, a regression model was used with WMH volume as the dependent variable and CVRF score as the independent variable, controlling for age, sex, and A/T pathology. In addition, we investigated the same association but this time excluding A/T group distinction as a covariate. Differences in WMH volume was analyzed for each CVRF score, one including history of hypertension and the other excluding history of hypertension as a risk factor due to limited hypertension data. Finally, each individual CVRF was compared to evaluate each of their potential impacts on WMHs. A similar linear regression model was used to observe potential age and sex differences for CVRF accumulation and WMH burden.

Several secondary analyses were completed to evaluate additional risk factors or hallmarks of AD. A separate regression was completed assessing the relationship between β-amyloid and WMH volume including homozygous APOE-*ε4* as a covariate. We further tested APOE-*ε4* by analyzing the interaction between β-amyloid and APOE-*ε4* genotype on WMH. Cognitive assessment measures (MOCA, MMSE, and Global CDR) were included as covariates in separate regression models to evaluate their impact on the association between WMH and β-amyloid. We additionally used linear regression models to observe whether cognitive diagnosis (CN, MCI, or AD) predicted WMH volume. Lastly, hippocampal volume fraction was used as a measure of atrophy. Two regression models with WMH volume and β-amyloid as independent variables were used with hippocampal volume fraction as the dependent variable, controlling for age, sex, years of education, and scanner manufacturer. Finally, hippocampal volume fraction was included as a covariate in the original regression model assessing the relationship between β-amyloid and WMH volume to determine possible effects.

Correlational analysis was used to assess the relationship between

increased WMH count, Aβ and Tau SUVR. WMH count was the dependent variable while Aβ SUVR was the independent variable, controlling for age, sex, years of education, and scanner manufacturer. This same method was used with Tau SUVR as the independent variable. Correlations between global β-amyloid association and WMH count were also assessed within A/T groups. Cohen's *d* effect size was also used to assess mean differences of WMH count across groups. Similar analyses were used to test the effects of APOE-*ε4* with WMH count as mentioned above with WMH volume by completing an additional regression including APOE-*ε4* as a covariate.

For localized cortical regional analysis, Pearson correlation was used to measure the relationship between gray matter β-amyloid PET SUVR and underlying WMH count from MRI in all brain regions. Significant regional associations were further investigated with ANOVA, controlling for age and sex to eliminate any biases. Finally, the same model was used on the subsets of pathological A/T groups, determining if any groups showed more localized regional differences than others. These results highlight potential localized associations between β-amyloid aggregation and WMH counts. The Benjamini-Hochberg procedure with a false discovery rate of 0.05 was used to correct for multiple comparisons in each of the regional analyses. This same method of analysis was used to test the relation between WMH volume distribution and cognitive scores. White matter independent regional analysis results were visualized using the Quantitative Imaging Toolkit (QIT; Cabeen et al., 2018).

3. Results

3.1. Influence of age and sex on WMH volume, β-amyloid accumulation, and CVRFs

Age was found to be a predictor of hypertension, systolic blood pressure, diastolic blood pressure, WMH volume, and β-amyloid (**Supplemental** Table S1**)**. Age had a positive relationship with hypertension, systolic blood pressure, WMH volume, and β-amyloid, but had a negative relationship with diastolic blood pressure. Sex was found to be a predictor of pulse rate, BMI, and cumulative CVRF scores, both including hypertension and excluding hypertension (**Supplemental Table S2**). Compared to females, male sex showed higher pulse rate, BMI, and both CVRF scores. Hypertension was excluded from the second cumulative score due to the dataset lacking hypertension measurements for many participants.

3.2. Relationship between WMH volume and AD pathology

The percentage of white matter volume occupied by WMH was significantly and positively correlated with β-amyloid PET SUVR (Fig. 1; $r = 0.28$, $p < 0.001$). We observed WMH volume to significantly predict global amyloid accumulation when controlling for age, sex, years of education, and scanner manufacturer ($F(1, 309) = 13.9$, $p = 0.0002$). We tested the distribution of WMH volume and found a skewed distribution (p = 1.18e-10). The correlational analyses were repeated after log transformation of WMH volume and outcomes remained the same, resulting in a significant positive correlation between WMH volume and β-amyloid ($r = 0.24$, p = 4.9e-5), and a nonsignificant positive correlation between WMH volume and metatemporal tau ($r = 0.09$, $p = 0.12$).

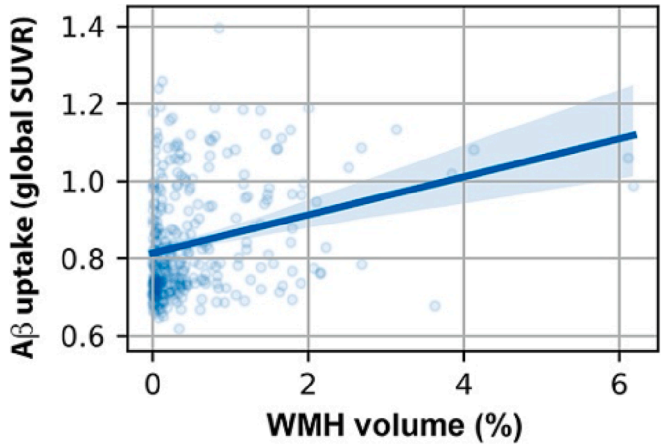

Fig. 1. Correlation between white matter hyperintensity volume and global β-amyloid standard uptake value ratio in all participants ($r = 0.28$, $p < 0.001$).

When including APOE genotype as a covariate, the results were remained significant ($F(1, 294) = 13.0$, $p = 0.0004$). Inclusion of MOCA, MMSE, and Global CDR, as covariates did not change the significant relationship between WMH volume and β-amyloid. We observed a significant effect of hippocampal volume fraction on WMH volume ($F(1, 580) = 16.9$, p = 4.5e-5) and β-amyloid ($F(1, 309) = 32.5$, p = 2.8e-8). Inclusion of hippocampal volume fraction in the regression model assessing the effect of WMH volume on β-amyloid did not alter significance ($p = 0.05$). We also found that WMH volume is predicted by CN $F(1, 580) = 8.12$, p = 4.5e-3) and MCI $F(1, 580) = 5.74$, $p = 0.02$) diagnoses, while AD does not $F(1, 580) = 0.954$, $p = 0.329$).

WMH volume percent of participants with either amyloid (A +) or tau (T +) pathology was higher than controls (A-/T-) (Fig. 2). We observed a significantly higher WMH percent in AD pathology participants (A+/T +) compared to controls (A-/T-) ($p = 0.007$, Cohen's d = 0.4, t = -2.5). Participants with Amyloid positive but Tau negative (A+/T-) also had higher WMH volume compared to controls ($p = 0.002$, Cohen's $d = 0.5$, t = -3.5). Only 12 participants were classified as A-/T + and had marginally higher WMH volume than controls ($p = 0.02$, Cohen's $d = 0.9$, t = -3.0). After testing for normality and performing a log transformation, mean differences between controls (A-/T-) and pathological groups remained the same [Amyloid positive, Tau negative (A+/T-; ($p = 0.012$, Cohen's $d = 0.36$, t = -2.5); Amyloid negative, Tau positive (A-/T+; ($p = 0.02$, Cohen's $d = 0.71$, t = -2.3); Amyloid positive, Tau positive (A+/T+; $p = 0.03$, Cohen's $d = 0.35$, t = -2.2)].

When correlation between the amount of WMH volume and amyloid was assessed across different groups (Fig. 3**A**), we observed significant positive correlation between WMH and amyloid in the A+/T- group (r = 0.36, $p < 0.001$). A marginal positive correlation was observed among A-/T + participants ($r = 0.58$, $p = 0.0498$), and the correlation trended toward significance among the A+/T + group ($r = 0.23$, $p = 0.09$). No significant association was found in the A-/T- group ($r = 0.06$, $p = 0.45$). A significant positive correlation was observed between β-amyloid SUVR and WMH count in the A+/T + group only. We observed neither a correlation nor an association between WMH and Tau uptake in the entire cohort (Fig. 4: correlation $p = 0.25$; association $p = 0.4$, controlling for age, sex, years of education and scanner manufacturer). These results were mostly maintained when controlling for age, sex, scanner, and years of education. The A-/T + group, initially holding a marginally significant relationship, was no longer significant after adjusting for covariates ($p = 0.214$, $R^2 = 0.202$, $B = 2457.6$), while the A+/T- group remained significant ($p = 0.008$, $R^2 = 0.209$, $B = 2135.4$). Both the A+/T+ ($p = 0.934$, $R^2 = 0.199$, $B = 79.6$) and the A-/T- remained insignificant after including covariates (p = 0079, $R^2 = 0.204$, B = -1155.5).

We additionally tested the distribution of WMH volume across groups. Our results showed the A-/T- ($p = 1.81$), A-/T+ ($p = 0.28$), and A+/T- ($p = 1.95$) groups to be normally distributed, while the A+/T + group was not normally distributed ($p < 0.001$). A logarithmic transformation was performed for the WMH volume of the A+/T + group. Upon this transformation, the correlation between WMH volume and β-amyloid remained non-significant ($r = 0.19$, $p = 0.168$). When controlling for age, sex, scanner, and years of education, the result was significant ($p = 0.03$, $R^2 = 0.119$, $B = 1.39$).

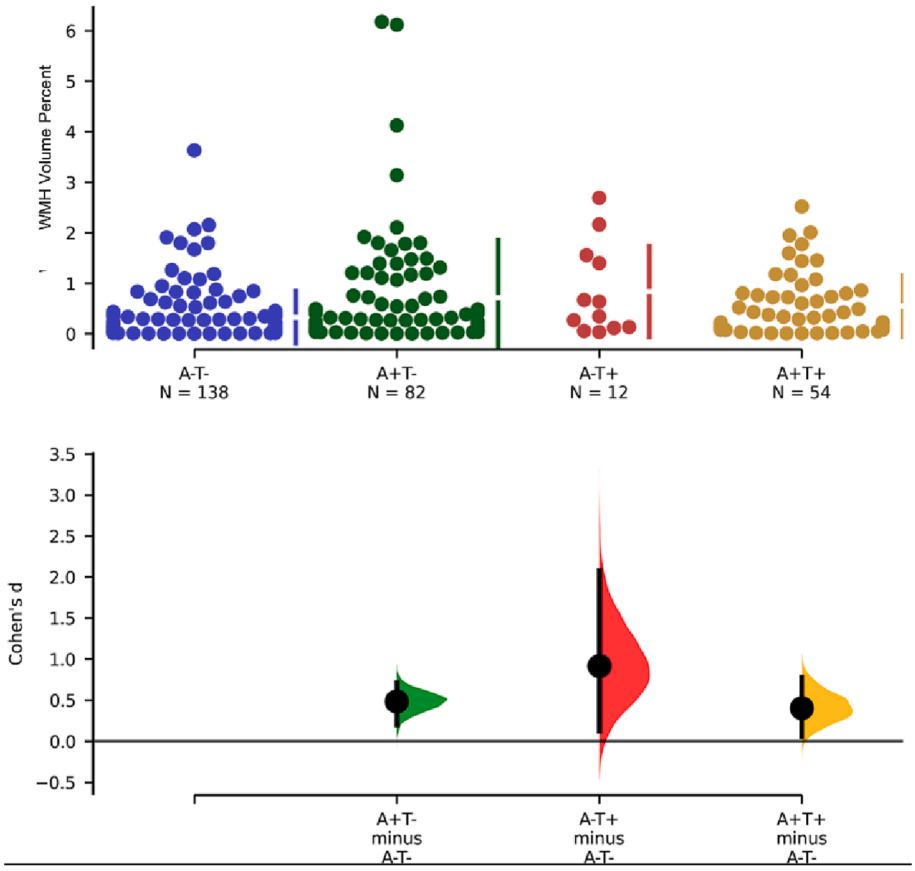

Fig. 2. Mean WMH volume differences between Amyloid negative, Tau negative (A-/T-) participants and participants with different pathology status: Amyloid positive, Tau negative (A+/T-; ($p = 0.002$, Cohen's $d = 0.5$); Amyloid negative, Tau positive (A-/T+; ($p = 0.02$, Cohen's $d = 0.9$); Amyloid positive, Tau positive (A+/T+; $p = 0.007$, Cohen's $d = 0.4$).

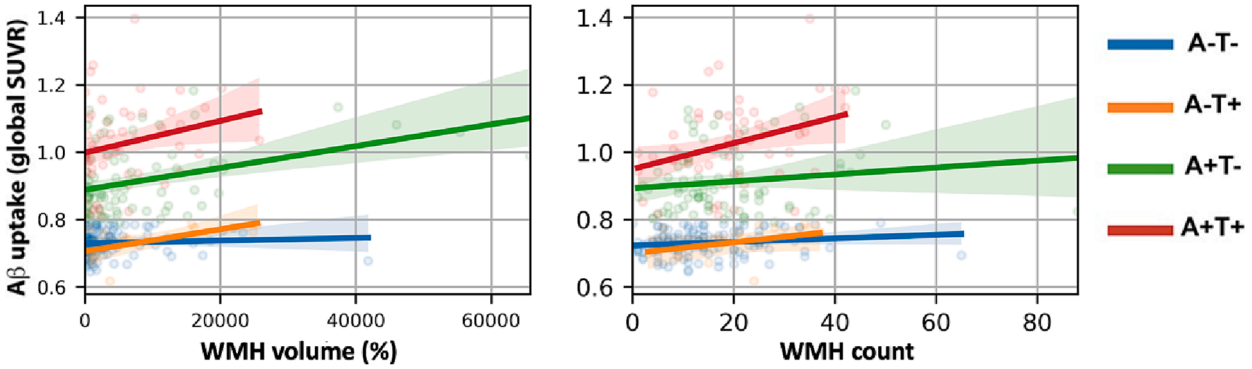

Fig. 3. A. Correlation between White matter hyperintensities (WMH) volume correlation and global Amyloid uptake among different pathology groups. Significant positive correlation in A+/T- ($r = 0.36$, $p < 0.001$), marginal positive correlation in A-/T+ ($r = 0.58$, $p = 0.0498$), nonsignificant correlation in A+/T+ ($r = 0.23$, $p = 0.09$), and no significant correlation in A-/T- ($r = 0.06$, $p = 0.45$). **B.** Correlation between WMH count and global Amyloid uptake among different pathology groups. Nonsignificant positive correlations in A+/T- ($r = 0.14$, $p = 0.22$), A-/T+ ($r = 0.35$, $p = 0.27$), and A-/T- ($r = 0.17$, $p = 0.07$). A significant positive association in A+/T+ ($r = 0.33$, $p = 0.01$).

3.3. Relationship between AD pathology and WMH count

A correlation analysis was used to observe the relationship between WMH count, as an alternate WMH measure, and both β-amyloid and tau uptake throughout the brain. First, WMH volume and count were significantly correlated ($r = 0.483$, $p = 3.99e\text{-}18$). Controlling for age, sex, years of education, and scanner manufacturer, Aβ SUVR was significantly associated with increased WMH count (Fig. 5**A**; $p < 0.001$, $r = 0.25$). This result remained significant when including APOE genotype as a covariate ($F(1, 263) = 11.9$, $p = 0.0007$) though there was no significant interaction between Aβ and APOE in predicting WMH count ($F(4, 259) = 1.27$, $p = 0.3$). Tau SUVR was also significantly associated with increased WMH count (Fig. 5**B**; $p = 0.02$, $r = 0.11$). When comparing correlation between global β-amyloid accumulation and WMH count among differing pathological groups, the results were similar to the analysis of WMH volume (Fig. 3**B**). There was a significant positive correlation between WMH count and Aβ SUVR in the A+/T + group ($r = 0.33$, $p = 0.01$). The correlation was not significant in the A-/

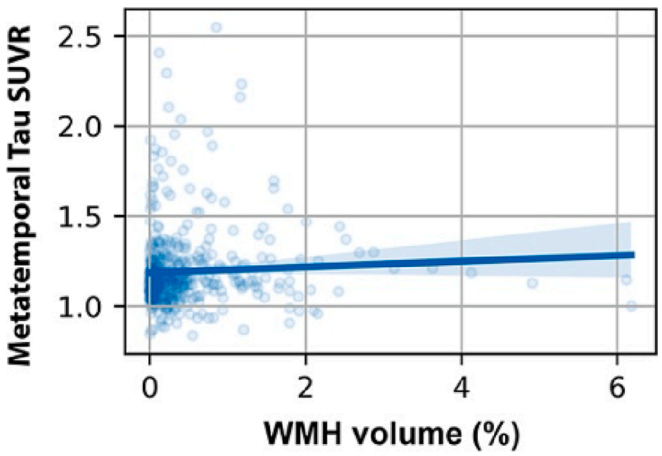

Fig. 4. Correlation between white matter hyperintensities (WMH) volume and *meta*-temporal Tau standard uptake value ratio (correlation $p = 0.25$; association $p = 0.4$).

T + group ($r = 0.35$, $p = 0.27$), and the A-/T- and A+/T- group trended toward significance with a slightly positive correlation (A-/T-: $r = 0.17$, $p = 0.07$; A+/T-: $r = 0.14$, $p = 0.22$). Overall, we observed significantly higher WMH count in participants with either A + or T + pathology compared to controls (Fig. 6). Compared to controls, WMH count was significantly higher in the AD group (A+/T +) ($p = 0.001$, Cohen's $d = 0.5$), the A+/T- group ($p = 0.007$, Cohen's $d = 0.4$) and the A-/T + group ($p = 0.04$, Cohen's $d = 0.6$). When assessing WMH count distribution A-/T- ($p = 1.40$), A+/T+ ($p = 0.89$), A+/T- ($p = 0.06$) groups were all normally distributed. As a result of the limited sample size in the A-/T + group normality could not be determined. However, since the A-/T + group represents non-AD pathology, this exclusion is justified. Inclusion of MOCA, MMSE, and Global CDR, as covariates did not change the significant relationship between WMH count and β-amyloid.

3.4. Regional associations between WMH burden and AD pathology

In order to assess the relationship between the spatial distribution of AD pathology and WMH burden, further regional analysis compared the association of average PET SUVR of β-amyloid in the gray matter with WMH volume measurements from MRI within the underlying corresponding white matter region. The results of the Pearson correlation that showed a significant association between PET SUVR and WMH volume in regions averaged across hemispheres were observed in the precentral ($r = 0.16$, $p = 0.007$), caudal middle frontal ($r = 0.12$, $p = 0.04$), cuneus ($r = 0.17$, $p = 0.003$), fusiform ($r = 0.18$, $p = 0.002$), inferior parietal ($r = 0.12$, $p = 0.04$), isthmus cingulate ($r = 0.13$, $p = 0.02$), lateral occipital ($r = 0.17$, $p = 0.004$), lingual ($r = 0.19$, $p = 0.001$), paracentral ($r = 0.12$, $p = 0.05$), pericalcarine ($r = 0.12$, $p = 0.04$), precuneus ($r = 0.13$, $p = 0.02$), superior parietal ($r = 0.15$, $p = 0.01$), and supramarginal ($r = 0.14$, $p = 0.01$) regions (**Supplemental Table S3**). After running a multiple comparison correction, the regions that survived and remained significantly associated were the precentral, cuneus, fusiform, isthmus cingulate, lateral occipital, lingual, superior parietal, and supramarginal regions. When further controlling for age and sex after multiple comparison correction, none remained significant.

The Pearson correlation results for regional association between average PET SUVR of β-amyloid in gray matter with WMH volume measurements in each hemisphere are visualized in Fig. 7**,** with the most significant regions indicated by a red arrow. Without averaging across both hemispheres, the regions that were no longer significantly associated were the inferior parietal ($r = 0.1$, $p = 0.09$), paracentral ($r = 0.12$, $p = 0.051$), and pericalcarine ($r = 0.11$, $p = 0.06$) regions. However, the middle temporal ($r = 0.18$, $p = 0.002$), pars orbitalis ($r = 0.17$, $p = 0.004$), and posterior cingulate ($r = 0.12$, $p = 0.04$) regions became significant when only assessing the right hemisphere. The results of the Pearson correlation in the left hemisphere showed that the caudal middle frontal ($r = 0.07$, $p = 0.25$), isthmus cingulate ($r = 0.09$, $p = 0.12$), and paracentral ($r = 0.099$, $p = 0.09$) regions were no longer significantly correlated. There were no additional regions that appeared significant in this hemisphere alone. The frontal pole in both hemispheres was disregarded due to absence of data in one participant. The right hemisphere was also missing data in the medial orbitofrontal region. The results for the association between cognitive score and WMH special distribution can be found in the Supplemental Material.

3.5. Relationship between APOE genotype and WMH burden

Including APOE genotype as a covariate when assessing the relationship between β-amyloid and WMH volume did not alter significance. Homozygous APOE *ε4/ε4* genotypes did predict global WMH volume when controlling for age and sex, though there were only 14 participants with this genotype ($F(1, 282) = 3.94$, $p = 0.0.048$, $\beta = 0.36$). However, the presence of one or more APOE-*ε4* alleles was not predictive of WMH volume ($F(1, 282) = 0.13$, $p = 0.72$, $\beta = -0.034$). In testing the interaction between APOE genotypes and β-amyloid in predicting WMH volume, there was a significant result ($F(4, 290) = 2.89$, $p = 0.03$) specifically the APOE *ε3/ε3* homozygous genotype ($p = 0.038$, $\beta =$

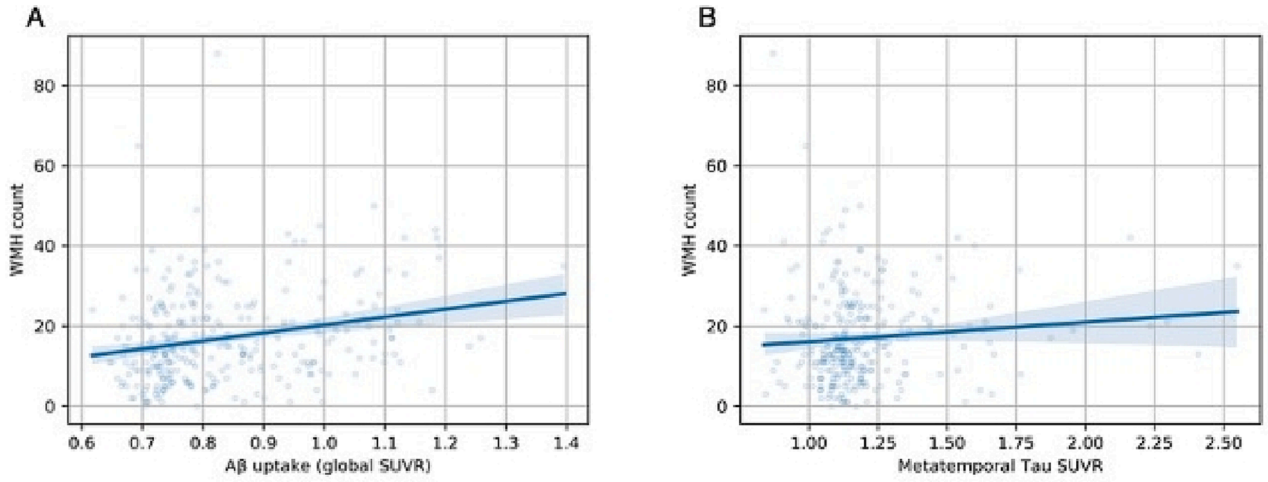

Fig. 5. A. Correlation between white matter hyperintensity (WMH) count and global Amyloid standard uptake value ratio ($p < 0.001$, $r = 0.25$). **B.** Correlation between white matter hyperintensity (WMH) count and *meta*-temporal Tau standard uptake value ratio ($p = 0.02$, $r = 0.11$).

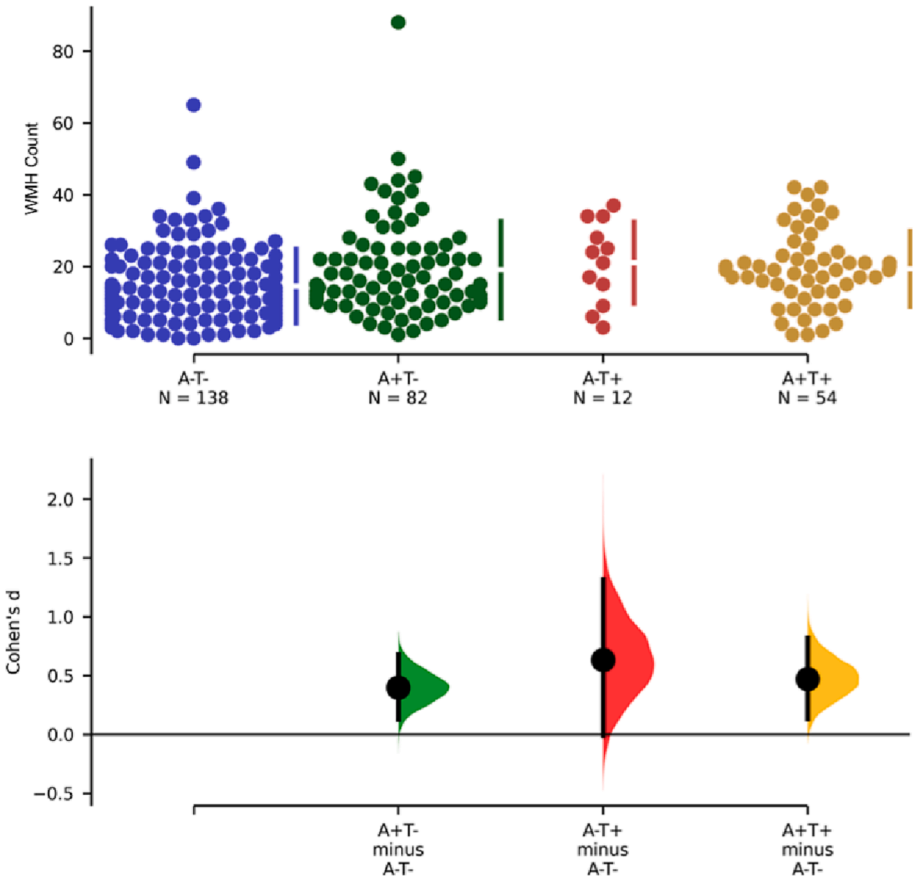

Fig. 6. Mean WMH count differences between groups. Amyloid positive, tau positive (A+/T+; $p = 0.001$, Cohen's $d = 0.5$); Amyloid positive, tau negative (A+/T-; $p = 0.007$, Cohen's $d = 0.4$); Amyloid negative, tau positive (A-/T+; $p = 0.04$, Cohen's $d = 0.6$).

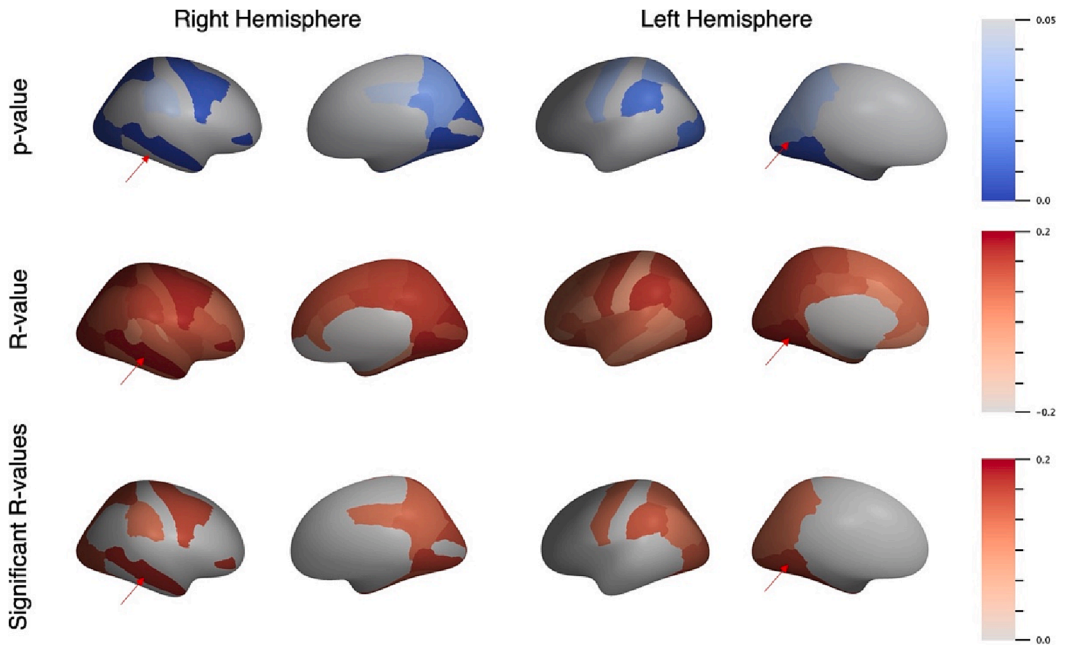

Fig. 7. Regional Pearson correlation between β-amyloid uptake and white matter hyperintensities in left and right hemispheres, showing p-values, R-values, and only significant R-values ($p < 0.05$). The most statistically significant regions are indicated by red arrows. Right hemisphere: middle temporal ($p = 0.002$, $R = 0.18$); Left hemisphere: fusiform ($p = 0.005$, $R = 0.017$). (For interpretation of the references to colour in this figure legend, the reader is referred to the web version of this article.)

4.13e + 04). Overall, the interaction effects did not alter the significance of β-amyloid predicting WMH volume ($F(1, 290) = 13.37$, $p = 0.0003$).

When controlling for APOE genotype in the relationship between β-amyloid and WMH count, the results remained significant ($F(1, 263) = 11.9$, $p = 0.0007$). There was no significant interaction between β-amyloid and APOE in predicting WMH count ($F(4, 259) = 1.27$, $p = 0.28$). Lastly, homozygous APOE *ε4/ε4* did not predict WMH count ($F(1, 282) = 0.11$, $p = 0.74$).

3.6. Relationship between CVRFs and WMH burden

Ordinary least squares regression analysis was used to assess the effect of CVRFs on WMH volume. The cumulative CVRF score including and excluding hypertension as a risk factor were not associated with increased WMH volume ($p = 0.34$, $R^2 = 0.15$, $t = 0.95$ and $p = 0.98$, $R^2 = 0.18$, $t = 0.025$, respectively). Additionally, no individual CVRF was associated with WMH volume (**Supplemental Table S4**).

4. Discussion

The goal of this study is to further understand the relationship between Alzheimer's Disease pathologies and WMHs and how they spatially align across the brain. Since vasculopathy likely plays a role in WMHs, we analyzed CVRFs to assess their potential relationship with lesion accumulation. Our findings show a strong relationship between increased β-amyloid deposition and WMHs globally. Individuals with AD pathological categorization (A+/T +) showed the highest WMH volume, aligning with literature linking WMH with AD (Grimmer et al., 2012, Provenzano et al., 2013, Lee et al., 2016, Birdsill et al., 2014., Hirono et al., 2000). Although we were unable to demonstrate CVRFs as a predictor of WMHs, we did observe significant age and sex differences across CVRFs. Finally, the colocalization of β-amyloid and WMHs in brain regions significant for early-stage AD suggest that both may be associated with eventual cognitive decline. Overall, the association between β-amyloid and WMHs may relate to the vascular origins of neurodegeneration and future studies should continue to investigate the mechanisms and downstream effects that contribute to this relationship.

In support of previous literature (Duanping et al., 1996), we found age was a strong predictor of both WMH volume and AD pathology. We also found WMH burden had a strong positive relationship with amyloid accumulation, but not tau deposition, which also confirms findings from previous studies (Graff-Radford et al. 2019, Grimmer et al. 2012). The lack of association between WMH burden and tau suggests that the neurodegenerative mechanisms that contribute to hyperphosphorylated tau in the brain may not be directly vascular in origin and may instead exert its effects differently, though this hypothesis needs further testing (Canepa and Fossati, 2021). Specifically, participants in groups with amyloid (A +) pathologies had higher mean WMH volumes than those without amyloid pathologies. These findings are consistent with autopsy studies showing correlations between CAA and WMHs (Chen et al. 2019). It is well known that WMHs, particularly when located in subcortical structures, are associated with hypertensive arteriolosclerosis (Charidimou et al 2016). However, the combination of WMHs and a positive amyloid PET scan raises the possibility of underlying CAA. The most significant positive association with WMHs was within the group of Alzheimer's pathologic change (A+/T-), which is on the AD continuum but not considered AD, as defined by Jack et al., 2018. Since many participants in this sample are CN, this significant positive relationship may be present in those with age-related WMH accumulation not affecting cognition. Additionally, this group contained a few participants with much higher WMH volumes than in other groups. The A+/T- group is defined as generally asymptomatic, though at risk for AD (Jack et al., 2016).

Inclusion of cognitive scores MMSE, MOCA, and Global CDR had no effect on the associations found between β-amyloid and WMH volume, therefore not significantly impacting this relationship. In the literature, worse performance on these cognitive tests has been associated with increased WMH volume (Wang et al., 2020). Additionally, WMH volume was only predicted by CN and MCI diagnoses, not AD. The relationship between WMH volume often predicts AD in the preclinical stages, likely accounting for the relationship we observed (Mortamais et al., 2014; Brickman, 2013). The relationship between higher MMSE scores and increased WMH volume showed significance with multiple comparison correction while controlling for age and sex in the isthmus cingulate region. For Global CDR scores, this spatial distribution was significant in the isthmus cingulate, temporal pole, and pars triangularis. Lastly, the MOCA scores showed significant positive spatial relationships in the isthmus cingulate, lingual, and temporal pole regions. The literature states that WMHs and cortical structure instability in certain brain regions may have larger effects on certain aspects of cognition such as executive function, motor function, etc. (Lampe et al., 2019; Wu et al., 2021).

We also did not observe any significant effect of APOE-*ε4* presence on the established relationship between β-amyloid and WMH volume or WMH count. We did however observe a significant positive relationship between the presence of homozygous APOE-*ε4* alleles and WMH volume, which contributes to the idea that APOE-*ε4* may affect brain vasculature (Lyall et al., 2020; Sudre et al., 2017). Although, we did have a small sample size of individuals with the homozygous APOE-*ε4* genotype. Lastly, in using hippocampal volume fraction as a measure of atrophy, there was no change in significance of the association found between β-amyloid and WMH volume when including this as a covariate. We did observe hippocampal volume fraction predicting both WMH volume and β-amyloid SUVR. Increased hippocampal atrophy has been linked to WMHs primarily before grey matter changes (Fiford et al., 2017; Chételat, 2010). Because of this, increased hippocampal atrophy has been identified as an early AD pathological marker and has significant effects on cognitive performance (Jack et al., 2010; Svenningsson et al., 2019).

WMH volume in groups with differing AD pathology was not predicted by CVRFs, including individual risk factors and cumulative risk factor scores. We repeated a similar analysis excluding history of hypertension as a CVRF, due to the limited hypertension measurements within our dataset, and maintained the same null finding. The lack of statistical power due to the small sample size in this subset of the data with hypertension information as well as the cross-sectional nature may also be reasons for the lack of an association between CVRFs and WMHs, despite a significant association between WMHs and β-amyloid. Additionally, many other datasets include risk factors such as cholesterol, diabetes, smoking, among others to be more comprehensive in their cardiovascular risk assessment (Luchsinger et al., 2005, Gottesman et al., 2017, Debette et al., 2011). The subjects in our study did not have these metrics available, which limited the scope of CVRFs we could include and likely impacted our result. Another hypothesis as to these non-significant associations is the ADNI dataset containing an overall low vascular burden at baseline but high AD pathological burden, which does not reflect populations with high vascular risk (Lorius et al., 2015). Authors also suggest that CVRFs increase the risk of dementia in cognitively unimpaired individuals through increased WMH volume burden as an early mechanism and exert their effects preclinically, however we did not differentiate participants by disease stage (Krivanek et al., 2021; Kandel et al., 2016). We did not find an association between WMH volume and CVRFs globally, but a more specific regional analysis of poor cerebral blood flow and its potential colocalization of WMHs could better assess this hypothesis. Although we did not analyze the direct effects of CVRFs on β-amyloid in the brain, perhaps this is an area for future research, exploring how vascular irregularities cause β-amyloid and lesion accumulation.

Age and sex differences were also analyzed for CVRFs, WMH volume, and β-amyloid SUVR. The results indicated age as a predictor of hypertension, systolic and diastolic blood pressure, β-amyloid uptake, and increased WMH volume which aligns with the literature (Alqarni et al.

2021, Sachdev et al. 2009; Koran et al., 2017; Gannon et al. 2019). Sex differences were present for pulse rate, BMI, and cumulative CVRF scores. Cardiovascular sex differences are a result of both hormonal and non-hormonal factors, and likely contribute to the increased likelihood of females developing AD (Merz and Cheng, 2016, Arnold et al. 2017). Females tend to have greater longevity than males, and since age is a predictor of both AD and many of its risk factors, this is the major reason females have higher prevalence of AD (Beam et al. 2018). Our results suggest that these vascular risk factors are not predictive of brain lesions relating to AD or differing amyloid and tau pathologies. However, age and sex differences may contribute to the acquisition of various AD risk factors.

WMH count was used as another method of measuring WMH burden. WMH count has been used in the literature to quantify WMHs in several areas of neuroscience research, typically utilizing a minimum lesion diameter before considering the lesion a WMH (Williamson et al. 2018, Sardanelli et al. 2005). To assess WMH count as an added measure, we utilized the same multiple linear regression methods as those used for the association of WMH volume with β-amyloid and A/T pathological groups. Both statistical tests on the WMH volume and the WMH count showed similar results, confirming that WMH count is an accurate measure to use alongside WMH volume. Correlations of WMH count with β-amyloid within A/T pathological groups also paralleled the WMH volume analysis result.

Several studies have investigated the association between regional β-amyloid accumulation and WMHs, though the basis of this relationship is not completely understood (Weaver et al. 2019, Grimmer et al. 2012). Our regional analysis showed that β-amyloid and WMH accumulation in the precentral, cuneus, fusiform, isthmus cingulate, lateral occipital, lingual, superior parietal, and supramarginal regions were most significantly associated across all pathological groups when averaged across hemispheres. Variation in the locations of increased WMHs are indicative of AD and its phase of progression, some of these regions being more implicated in cognitive decline than others (Brickman et al. 2009, Kao et al. 2019; Söderlund et al., 2006). Early stages of AD before severe symptom onset are associated with increased β-amyloid accumulation in the neocortex, regions which were significantly associated with WMHs in our analysis (Palmqvist et al. 2017, Thal et al. 2002, Moscoso et al. 2020). This may be due in part to effects of CAA on perfusion. Regions important in early AD showed β-amyloid accumulation in the precuneus, medial orbitofrontal, and posterior cingulate, which are part of the functional MRI resting state Default Mode Network and play a significant role in memory (Palmqvist et al., 2017, Sperling et al., 2009). Several studies state that anterior WMH accumulation facilitates normal age-related cognitive decline, while a posterior distribution may be more linked to AD (Brickman et al., 2009, Weaver et al., 2019). Considering the predisposition of CAA for posterior cortical brain regions, this is also consistent with the development of CAA there playing a role in WMH. Specifically, higher WMH volumes were observed in the splenium of the corpus callosum and posterior periventricular regions in individuals diagnosed with AD (Yoshita et al., 2006). Cognition is affected differently based on the location of WMHs, with lower executive functioning with WMH burdens in frontal areas, and lower memory performance due to WMH burden in deep frontal and occipital regions (Brugulat-Serrat et al., 2020). Our results indicate that in brain regions that may be implicated in Alzheimer's related cognitive decline, β-amyloid colocalizes with WMHs (Li et al. 2015).

Because WMHs likely indicate the presence of cerebral small vessel disease, the presence of WMHs may inhibit proper clearance of β-amyloid plaques and could result in β-amyloid deposition in the brain, also known as the two-hit vascular hypothesis (Kisler et al., 2017, Grimmer et al. 2012). B-amyloid accumulation in the brain causes impaired cerebral blood flow to the neocortex, even before AD symptoms are present, which may ultimately lead to lesions such as WMHs (Iadecola, 2003). Therefore, the presence of β-amyloid and WMHs in the brain may represent a feedback loop that facilitates the development of AD. Our results do indicate a regional association between β-amyloid and WMHs, though our findings are not sufficient to reaffirm the two-hit vascular hypothesis. Researchers have hypothesized that WMHs localize in regions with the greatest vascular pathology and metabolic dysfunction, most often in posterior regions for individuals with AD (Zhu et al. 2012, Weaver et al. 2019, Brickman et al. 2012).

The results of our study were limited due to the ADNI dataset, which is not ideal for assessing vascular risk and limited our sample size. It is well studied that hypertension does have vascular effects in the brain, however we were unable to replicate this result with our given dataset (Duanping et al., 1996; Gottesman et al. 2010). Inclusion of additional vascular risk factors known to increase likelihood of AD such as diabetes, hyperlipidemia, and hypercholesterolemia would have strengthened these results, however these were not collected and reported in the dataset. Additionally, one of our pathological groups (A-/T +) had significantly fewer participants compared to the rest of the groups, which decreases the reliability of results. Though since the A-/T + pathology is a result of non-Alzheimer's pathologic change, and is therefore less relevant to our objective of assessing risk factors and WMHs related to AD. Last, a longitudinal approach would be ideal in determining the impacts of CVRFs on AD pathology over time, however data indicating the time of the initial appearance of participants' CVRFs was not available.

5. Conclusion

Our results show a clear association between β-amyloid and WMH accumulation especially in regions implicated in cognitive decline, although the mechanism of this association is still not fully understood. The positive association between amyloid positive (A +) pathological groups and WMH volume highlights vascular lesion formation, potentially mediated by CAA. We found hippocampal volume to predict both WMH volume and β-amyloid, adding to the idea of hippocampal atrophy as a possible early marker for disease. Inclusion of APOE genotype into the relationship between β-amyloid and WMH showed no effect, but homozygous APOE-*ε4* genotypes predicted WMH volume. Additionally, addition of various measures of cognitive ability did noy alter the relationship between WMHs and β-amyloid. Though we did not observe any relationship between CVRFs and β-amyloid or WMH volume, repeating this analysis with other factors shown to increase AD risk such as diabetes, smoking, and cholesterol may yield a different result. With many participants in the study mostly cognitively normal but still presenting with pathological levels of β-amyloid, tau, and WMHs, our results give insight into the early stage of the disease and possible early signs of later disease severity. Specifically, the spatial co-occurrences found between β-amyloid and WMHs may be indicative of disease stage. These findings highlight potential causes of AD and the mechanisms by which they occur as targets for future preventions and treatments.

CRediT authorship contribution statement

Sierra Alban: Conceptualization, Methodology, Formal analysis, Investigation, Data curation, Writing – original draft, Writing – review & editing. **Kirsten M. Lynch:** Validation, Writing – original draft, Writing – review & editing. **John M. Ringman:** Validation, Writing – original draft. **Arthur W. Toga:** Supervision, Writing – review & editing. **Helena C. Chui:** Validation, Writing – original draft. **Farshid Sepehrband:** Conceptualization, Methodology, Software, Validation, Formal analysis, Resources, Data curation, Writing – original draft, Writing – review & editing, Supervision, Project administration. **Jeiran Choupan:** Conceptualization, Methodology, Validation, Formal analysis, Resources, Data curation, Writing – original draft, Writing – review & editing, Supervision, Project administration.

Declaration of Competing Interest

The authors declare that they have no known competing financial interests or personal relationships that could have appeared to influence the work reported in this paper.

Data availability

In order to access Alzheimer's Disease Neuroimaging Initiative (ADNI) data, individuals must apply before access is granted.

Acknowledgement

This work was supported by NIH grants: 2P41EB015922-21,1P01AG052350-01 and USC ADRC 5P50AG005142 and 1P30AG066530-01. This research reported in this publication was also supported by the National Institute of Mental Health, and National Institute of Aging of the NIH under Award Numbers RF1MH123223, and R01AG070825. KML is supported by the National Institute on Aging (NIA) of the NIH Institutional Training Grant T32AG058507. The content is solely the responsibility of the authors and does not necessarily represent the official views of the NIH. ADNI: Data collection and sharing for this project was funded by the Alzheimer's Disease Neuroimaging Initiative (ADNI) (National Institutes of Health Grant U01AG024904) and DOD ADNI (Department of Defense award number W81XWH-12-2-0012). ADNI is funded by the National Institute on Aging, the National Institute of Biomedical Imaging and Bioengineering, and through generous contributions from the following: AbbVie, Alzheimer's Association; Alzheimer's Drug Discovery Foundation; Araclon Biotech; Bio Clinica, Inc.; Biogen; Bristol-Myers Squibb Company; CereSpir, Inc.; Cogstate; Eisai Inc.; Elan Pharmaceuticals, Inc.; Eli Lilly and Company; EuroImmun; F. Hoffmann-LaRoche Ltd and its affiliated company Genentech, Inc.; Fujirebio; GE Healthcare; IXICO Ltd.; Janssen Alzheimer Immunotherapy Research & Development, LLC.; Johnson & Johnson Pharmaceutical Research & Development LLC.; Lumosity; Lundbeck; Merck & Co., Inc.; Meso Scale Diagnostics, LLC.; NeuroRx Research; Neurotrack Technologies; Novartis Pharmaceuticals Corporation; Pfizer Inc.; Piramal Imaging; Servier; Takeda Pharmaceutical Company; and Transition Therapeutics. The Canadian Institutes of Health Research is providing funds to support ADNI clinical sites in Canada. Private sector contributions are facilitated by the Foundation for the National Institutes of Health (www.fnih.org). The grantee organization is the Northern California Institute for Research and Education, and the study is coordinated by the Alzheimer's Therapeutic Research Institute at the University of Southern California. ADNI data are disseminated by the Laboratory for Neuro Imaging at the University of Southern California. The authors would like to thank Dr. Ryan P. Cabeen (Laboratory of NeuroImaging, USC Stevens Neuroimaging and Informatics Institute, Keck School of Medicine, University of Southern California, Los Angeles, CA, USA) for his help on using Quantitative Imaging Toolkit software.

Appendix A. Supplementary data

Supplementary data to this article can be found online at https://doi.org/10.1016/j.nicl.2023.103383.

References

Alqarni, A., Jiang, J., Crawford, J.D., Koch, F., Brodaty, H., Sachdev, P., Wen, W., 2021. Sex differences in risk factors for white matter hyperintensities in non-demented older individuals. Neurobiol. Aging 98, 197–204. https://doi.org/10.1016/j.neurobiolaging.2020.11.001.

Arnold, A.P., Cassis, L.A., Eghbali, M., Reue, K., Sandberg, K., 2017. Sex Hormones and Sex Chromosomes Cause Sex Differences in the Development of Cardiovascular Diseases. Arterioscler. Thromb. Vasc. Biol. 37, 746–756. https://doi.org/10.1161/ATVBAHA.116.307301.

Au, R., Massaro, J.M., Wolf, P.A., Young, M.E., Beiser, A., Seshadri, S., D'Agostino, R.B., DeCarli, C., 2006. Association of White Matter Hyperintensity Volume With Decreased Cognitive Functioning: The Framingham Heart Study. Arch. Neurol. 63, 246–250. https://doi.org/10.1001/archneur.63.2.246.

Avants, B., Tustison, N.J., Song, G., 2009. Advanced Normalization Tools: V1.0. 10.54294/uvnhin.

Baker, S.L., Maass, A., Jagust, W.J., 2017. Considerations and code for partial volume correcting [18F]-AV-1451 tau PET data. Data Br. 15, 648–657. https://doi.org/10.1016/j.dib.2017.10.024.

Beam, C.R., Kaneshiro, C., Jang, J.Y., Reynolds, C.A., Pedersen, N.L., Gatz, M., 2018. Differences Between Women and Men in Incidence Rates of Dementia and Alzheimer's Disease. J. Alzheimers. Dis. 64, 1077–1083. https://doi.org/10.3233/JAD-180141.

Birdsill, A.C., Koscik, R.L., Jonaitis, E.M., Johnson, S.C., Okonkwo, O.C., Hermann, B.P., LaRue, A., Sager, M.A., Bendlin, B.B., 2014. Regional white matter hyperintensities: aging, Alzheimer's disease risk, and cognitive function. Neurobiol. Aging 35, 769–776. https://doi.org/10.1016/j.neurobiolaging.2013.10.072.

Braak, H., Braak, E., 1991. Neuropathological stageing of Alzheimer-related changes. Acta Neuropathol. 82, 239–259. https://doi.org/10.1007/BF00308809.

Breteler, M.M., van Swieten, J.C., Bots, M.L., Grobbee, D.E., Claus, J.J., van den Hout, J. H., van Harskamp, F., Tanghe, H.L., de Jong, P.T., van Gijn, J., 1994. Cerebral white matter lesions, vascular risk factors, and cognitive function in a population-based study: the Rotterdam Study. Neurology 44, 1246–1252. 10.1212/wnl.44.7.1246.

Brickman, A.M., 2013. Contemplating Alzheimer's Disease and the Contribution of White Matter Hyperintensities. Curr. Neurol. Neurosci. Rep. 13, 415. https://doi.org/10.1007/s11910-013-0415-7.

Brickman, A.M., Muraskin, J., Zimmerman, M.E., 2009. Structural neuroimaging in Altheimer's disease: do white matter hyperintensities matter? Dialogues Clin. Neurosci. 11, 181–190. 10.31887/DCNS.2009.11.2/ambrickman.

Brickman, A.M., Provenzano, F.A., Muraskin, J., Manly, J.J., Blum, S., Apa, Z., Stern, Y., Brown, T.R., Luchsinger, J.A., Mayeux, R., 2012. Regional white matter hyperintensity volume, not hippocampal atrophy, predicts incident Alzheimer disease in the community. Arch. Neurol. 69, 1621–1627. https://doi.org/10.1001/archneurol.2012.1527.

Brugulat-Serrat, A., Salvadó, G., Sudre, C.H., Grau-Rivera, O., Suárez-Calvet, M., Falcon, C., Sánchez-Benavides, G., Gramunt, N., Fauria, K., Cardoso, M.J., Barkhof, F., Molinuevo, J.L., Gispert, J.D., 2020. Patterns of white matter hyperintensities associated with cognition in middle-aged cognitively healthy individuals. Brain Imaging Behav. 14 (5), 2012–2023.

Burton, E.J., Kenny, R.A., O'Brien, J., Stephens, S., Bradbury, M., Rowan, E., Kalaria, R., Firbank, M., Wesnes, K., Ballard, C., 2004. White Matter Hyperintensities Are Associated With Impairment of Memory, Attention, and Global Cognitive Performance in Older Stroke Patients. Stroke 35, 1270–1275. https://doi.org/10.1161/01.STR.0000126041.99024.86.

Cabeen, R. P., Laidlaw, D. H., and Toga, A. W. (2018). Quantitative Imaging Toolkit: Software for Interactive 3D Visualization, Data Exploration, and Computational Analysis of Neuroimaging Datasets. Proceedings of the International Society for Magnetic Resonance in Medicine (ISMRM), 2854.

Canepa, E., Fossati, S., 2021. Impact of Tau on Neurovascular Pathology in Alzheimer's Disease. Front. Neurol. 11, 573324 https://doi.org/10.3389/fneur.2020.573324.

Charidimou, A., Boulouis, G., Haley, K., Auriel, E., van Etten, E.S., Fotiadis, P., Reijmer, Y., Ayres, A., Vashkevich, A., Dipucchio, Z.Y., Schwab, K.M., Martinez-Ramirez, S., Rosand, J., Viswanathan, A., Greenberg, S.M., Gurol, M.E., 2016. White matter hyperintensity patterns in cerebral amyloid angiopathy and hypertensive arteriopathy. Neurology 86, 505–511. https://doi.org/10.1212/WNL.0000000000002362.

Chen, S.-J., Tsai, H.-H., Tsai, L.-K., Tang, S.-C., Lee, B.-C., Liu, H.-M., Yen, R.-F., Jeng, J.-S., 2019. Advances in cerebral amyloid angiopathy imaging. Ther. Adv. Neurol. Disord. 12, 1756286419844113. 10.1177/1756286419844113.

Chen, Y.W., Gurol, M.E., Rosand, J., Viswanathan, A., Rakich, S.M., Groover, T.R., Greenberg, S.M., Smith, E.E., 2006. Progression of white matter lesions and hemorrhages in cerebral amyloid angiopathy. Neurology 67 (1), 83–87.

Chételat, G., Villemagne, V.L., Bourgeat, P., Pike, K.E., Jones, G., Ames, D., Ellis, K.A., Szoeke, C., Martins, R.N., O'Keefe, G.J., Salvado, O., Masters, C.L., Rowe, C.C., Group, A.I.B. and L.R., 2010. Relationship between atrophy and β-amyloid deposition in Alzheimer disease. Ann. Neurol. 67, 317–324. 10.1002/ana.21955.

Cleveland Clinic. "Vital Signs." January 2019, Retrieved January 7, 2022, from https://my.clevelandclinic.org/health/articles/10881-vital-signs.

Conner, S.C., Pase, M.P., Carneiro, H., Raman, M.R., McKee, A.C., Alvarez, V.E., Walker, J.M., Satizabal, C.L., Himali, J.J., Stein, T.D., Beiser, A., Seshadri, S., 2019. Mid-life and late-life vascular risk factor burden and neuropathology in old age. Ann. Clin. Transl. Neurol. 6, 2403–2412. https://doi.org/10.1002/acn3.50936.

Convit, A., De Leon, M.J., Tarshish, C., De Santi, S., Tsui, W., Rusinek, H., George, A., 1997. Specific Hippocampal Volume Reductions in Individuals at Risk for Alzheimer's Disease. Neurobiol. Aging 18, 131–138. https://doi.org/10.1016/S0197-4580(97)00001-8.

Dadar, M., Camicioli, R., Duchesne, S., Collins, D.L., 2020. The temporal relationships between white matter hyperintensities, neurodegeneration, amyloid beta, and cognition. Alzheimer's Dement. (Amsterdam, Netherlands) 12, e12091. 10.1002/dad2.12091.

Corder, E.H., Saunders, A.M., Strittmatter, W.J., Schmechel, D.E., Gaskell, P.C., Small, G. W., Roses, A.D., Haines, J.L., Pericak-Vance, M.A., 1993. Gene Dose of Apolipoprotein E Type 4 Allele and the Risk of Alzheimer's Disease in Late Onset Families. Science (80- 261, 921–923. https://doi.org/10.1126/science.8346443.

Dale, A.M., Fischl, B., Sereno, M.I., 1999. Cortical Surface-Based Analysis: I. Segmentation and Surface Reconstruction. Neuroimage 9, 179–194. https://doi.org/10.1006/nimg.1998.0395.

de Leeuw, F.-E., Barkhof, F., Scheltens, P., 2004. White matter lesions and hippocampal atrophy in Alzheimer's disease. Neurology 62 (2), 310–312.

Debette, S., Seshadri, S., Beiser, A., Au, R., Himali, J.J., Palumbo, C., Wolf, P.A., DeCarli, C., 2011. Midlife vascular risk factor exposure accelerates structural brain aging and cognitive decline. Neurology 77, 461–468. https://doi.org/10.1212/WNL.0b013e318227b227.

DeCarli, C., Reed, T., Miller, B.L., Wolf, P.A., Swan, G.E., Carmelli, D., 1999. Impact of apolipoprotein E epsilon4 and vascular disease on brain morphology in men from the NHLBI twin study. Stroke 30, 1548–1553. https://doi.org/10.1161/01.str.30.8.1548.

Desikan, R.S., Ségonne, F., Fischl, B., Quinn, B.T., Dickerson, B.C., Blacker, D., Buckner, R.L., Dale, A.M., Maguire, R.P., Hyman, B.T., Albert, M.S., Killiany, R.J., 2006. An automated labeling system for subdividing the human cerebral cortex on MRI scans into gyral based regions of interest. Neuroimage 31, 968–980. https://doi.org/10.1016/j.neuroimage.2006.01.021.

Duanping, L., Lawton, C., Jianwen, C., Toole, J.F., Bryan, N.R., Hutchinson, R.G., Tyroler, H.A., 1996. Presence and Severity of Cerebral White Matter Lesions and Hypertension, Its Treatment, and Its Control. Stroke 27, 2262–2270. https://doi.org/10.1161/01.STR.27.12.2262.

Fiford, C.M., Manning, E.N., Bartlett, J.W., Cash, D.M., Malone, I.B., Ridgway, G.R., Lehmann, M., Leung, K.K., Sudre, C.H., Ourselin, S., Biessels, G.J., Carmichael, O.T., Fox, N.C., Cardoso, M.J., Barnes, J., Initiative, for the A.D.N.,, 2017. White matter hyperintensities are associated with disproportionate progressive hippocampal atrophy. Hippocampus 27, 249–262. https://doi.org/10.1002/hipo.22690.

Fischl, B., 2012. FreeSurfer. Neuroimage 62, 774–781. https://doi.org/10.1016/j.neuroimage.2012.01.021.

Fischl, B., Dale, A.M., 2000. Measuring the thickness of the human cerebral cortex from magnetic resonance images. Proc. Natl. Acad. Sci. 97, 11050–11055. https://doi.org/10.1073/pnas.200033797.

Fischl, B., Salat, D.H., Busa, E., Albert, M., Dieterich, M., Haselgrove, C., van der Kouwe, A., Killiany, R., Kennedy, D., Klaveness, S., Montillo, A., Makris, N., Rosen, B., Dale, A.M., 2002. Whole Brain Segmentation: Automated Labeling of Neuroanatomical Structures in the. Human Brain. Neuron 33, 341–355. https://doi.org/10.1016/S0896-6273(02)00569-X.

Fischl, B., Sereno, M.I., Dale, A.M., 1999. Cortical Surface-Based Analysis: II: Inflation, Flattening, and a Surface-Based Coordinate System. Neuroimage 9, 195–207. https://doi.org/10.1006/nimg.1998.0396.

Fischl, B., van der Kouwe, A., Destrieux, C., Halgren, E., Ségonne, F., Salat, D.H., Busa, E., Seidman, L.J., Goldstein, J., Kennedy, D., Caviness, V., Makris, N., Rosen, B., Dale, A.M., 2004. Automatically Parcellating the Human Cerebral Cortex. Cereb. Cortex 14, 11–22. https://doi.org/10.1093/cercor/bhg087.

Frangi, A.F., Niessen, W.J., Vincken, K.L., Viergever, M.A., 1998. Multiscale vessel enhancement filtering BT - Medical Image Computing and Computer-Assisted Intervention — MICCAI'98. In: Wells, W.M., Colchester, A., Delp, S. (Eds.), Springer. Berlin Heidelberg, Berlin, Heidelberg, pp. 130–137.

Gannon, O.J., Robison, L.S., Custozzo, A.J., Zuloaga, K.L., 2019. Sex differences in risk factors for vascular contributions to cognitive impairment & dementia. Neurochem. Int. 127, 38–55. https://doi.org/10.1016/j.neuint.2018.11.014.

Gottesman, R.F., Coresh, J., Catellier, D.J., Sharrett, A.R., Rose, K.M., Coker, L.H., Shibata, D.K., Knopman, D.S., Jack, C.R., Mosley Jr, T.H., 2010. Blood pressure and white-matter disease progression in a biethnic cohort: Atherosclerosis Risk in Communities (ARIC) study. Stroke 41, 3–8. https://doi.org/10.1161/STROKEAHA.109.566992.

Gottesman, R.F., Schneider, A.L.C., Zhou, Y., Coresh, J., Green, E., Gupta, N., Knopman, D.S., Mintz, A., Rahmim, A., Sharrett, A.R., Wagenknecht, L.E., Wong, D. F., Mosley, T.H., 2017. Association Between Midlife Vascular Risk Factors and Estimated Brain Amyloid Deposition. JAMA 317, 1443–1450. https://doi.org/10.1001/jama.2017.3090.

Graff-Radford, J., Arenaza-Urquijo, E.M., Knopman, D.S., Schwarz, C.G., Brown, R.D., Rabinstein, A.A., Gunter, J.L., Senjem, M.L., Przybelski, S.A., Lesnick, T., Ward, C., Mielke, M.M., Lowe, V.J., Petersen, R.C., Kremers, W.K., Kantarci, K., Jack, C.R., Vemuri, P., 2019. White matter hyperintensities: relationship to amyloid and tau burden. Brain 142, 2483–2491. 10.1093/brain/awz162.

Grimmer, T., Faust, M., Auer, F., Alexopoulos, P., Förstl, H., Henriksen, G., Perneczky, R., Sorg, C., Yousefi, B.H., Drzezga, A., Kurz, A., 2012. White matter hyperintensities predict amyloid increase in Alzheimer's disease. Neurobiol. Aging 33, 2766–2773. https://doi.org/10.1016/j.neurobiolaging.2012.01.016.

Gunning-Dixon, F.M., Raz, N., 2003. Neuroanatomical correlates of selected executive functions in middle-aged and older adults: a prospective MRI study. Neuropsychologia 41, 1929–1941. https://doi.org/10.1016/s0028-3932(03)00129-5.

Gurol, M.E., Irizarry, M.C., Smith, E.E., Raju, S., Diaz-Arrastia, R., Bottiglieri, T., Rosand, J., Growdon, J.H., Greenberg, S.M., 2006. Plasma beta-amyloid and white matter lesions in AD, MCI, and cerebral amyloid angiopathy. Neurology 66, 23–29. https://doi.org/10.1212/01.wnl.0000191403.95453.6a.

Hirono, N., Kitagaki, H., Kazui, H., Hashimoto, M., Mori, E., 2000. Impact of White Matter Changes on Clinical Manifestation of Alzheimer's Disease. Stroke 31, 2182–2188. https://doi.org/10.1161/01.STR.31.9.2182.

Ho, J., Tumkaya, T., Aryal, S., Choi, H., Claridge-Chang, A., 2019. Moving beyond P values: data analysis with estimation graphics. Nat. Methods 16, 565–566. https://doi.org/10.1038/s41592-019-0470-3.

Holland, C.M., Smith, E.E., Csapo, I., Gurol, M.E., Brylka, D.A., Killiany, R.J., Blacker, D., Albert, M.S., Guttmann, C.R.G., Greenberg, S.M., 2008. Spatial distribution of white-matter hyperintensities in Alzheimer disease, cerebral amyloid angiopathy, and healthy aging. Stroke 39, 1127–1133. https://doi.org/10.1161/STROKEAHA.107.497438.

Jack Jr, C.R., Wiste, H.J., Vemuri, P., Weigand, S.D., Senjem, M.L., Zeng, G., Bernstein, M.A., Gunter, J.L., Pankratz, V.S., Aisen, P.S., Weiner, M.W., Petersen, R. C., Shaw, L.M., Trojanowski, J.Q., Knopman, D.S., Initiative, the A.D.N.,, 2010. Brain beta-amyloid measures and magnetic resonance imaging atrophy both predict time-to-progression from mild cognitive impairment to Alzheimer's disease. Brain 133, 3336–3348. https://doi.org/10.1093/brain/awq277.

Jack Jr, C.R., Bennett, D.A., Blennow, K., Carrillo, M.C., Feldman, H.H., Frisoni, G.B., Hampel, H., Jagust, W.J., Johnson, K.A., Knopman, D.S., Petersen, R.C., Scheltens, P., Sperling, R.A., Dubois, B., 2016. A/T/N: An unbiased descriptive classification scheme for Alzheimer disease biomarkers. Neurology 87, 539–547. https://doi.org/10.1212/WNL.0000000000002923.

Iadecola, C., 2003. Cerebrovascular effects of amyloid-beta peptides: mechanisms and implications for Alzheimer's dementia. Cell. Mol. Neurobiol. 23, 681–689. https://doi.org/10.1023/a:1025092617651.

Jack, C.R., Bennett, D.A., Blennow, K., Carrillo, M.C., Dunn, B., Haeberlein, S.B., Holtzman, D.M., Jagust, W., Jessen, F., Karlawish, J., Liu, E., Molinuevo, J.L., Montine, T., Phelps, C., Rankin, K.P., Rowe, C.C., Scheltens, P., Siemers, E., Snyder, H.M., Sperling, R., Elliott, C., Masliah, E., Ryan, L., Silverberg, N., 2018. NIA-AA Research Framework: Toward a biological definition of Alzheimer's disease. Alzheimers Dement. 14 (4), 535–562.

Johnson, K.A., Schultz, A., Betensky, R.A., Becker, J.A., Sepulcre, J., Rentz, D., Mormino, E., Chhatwal, J., Amariglio, R., Papp, K., Marshall, G., Albers, M., Mauro, S., Pepin, L., Alverio, J., Judge, K., Philiossaint, M., Shoup, T., Yokell, D., Dickerson, B., Gomez-Isla, T., Hyman, B., Vasdev, N., Sperling, R., 2016. Tau positron emission tomographic imaging in aging and early Alzheimer disease. Ann. Neurol. 79, 110–119. https://doi.org/10.1002/ana.24546.

Kalaria, R.N., Akinyemi, R., Ihara, M., 2012. Does vascular pathology contribute to Alzheimer changes? J. Neurol. Sci. 322, 141–147. https://doi.org/10.1016/j.jns.2012.07.032.

Kamnitsas, K., Ledig, C., Newcombe, V.F.J., Simpson, J.P., Kane, A.D., Menon, D.K., Rueckert, D., Glocker, B., 2017. Efficient multi-scale 3D CNN with fully connected CRF for accurate brain lesion segmentation. Med. Image Anal. 36, 61–78. https://doi.org/10.1016/j.media.2016.10.004.

Kandel, B.M., Avants, B.B., Gee, J.C., McMillan, C.T., Erus, G., Doshi, J., Davatzikos, C., Wolk, D.A., 2016. White matter hyperintensities are more highly associated with preclinical Alzheimer's disease than imaging and cognitive markers of neurodegeneration. Alzheimer's Dement. Diagnosis. Assess. Dis. Monit. 4 (1), 18–27.

Kannel, W.B., McGee, D., Gordon, T., 1976. A general cardiovascular risk profile: The Framingham study. Am. J. Cardiol. 38, 46–51. https://doi.org/10.1016/0002-9149(76)90061-8.

Kao, Y.-H., Chou, M.-C., Chen, C.-H., Yang, Y.-H., 2019. White Matter Changes in Patients with Alzheimer's Disease and Associated Factors. J. Clin. Med. 8, 167. https://doi.org/10.3390/jcm8020167.

Kisler, K., Nelson, A.R., Montagne, A., Zlokovic, B.V., 2017. Cerebral blood flow regulation and neurovascular dysfunction in Alzheimer disease. Nat. Rev. Neurosci. 18, 419–434. https://doi.org/10.1038/nrn.2017.48.

Koran, M.E.I., Wagener, M., Hohman, T.J., 2017. Sex differences in the association between AD biomarkers and cognitive decline. Brain Imaging Behav 11, 205–213. https://doi.org/10.1007/s11682-016-9523-8.

Krivanek, T.J., Gale, S.A., McFeeley, B.M., Nicastri, C.M., Daffner, K.R., 2021. Promoting Successful Cognitive Aging: A Ten-Year Update. J. Alzheimers. Dis. 81, 871–920. https://doi.org/10.3233/JAD-201462.

Lampe, L., Kharabian-Masouleh, S., Kynast, J., Arelin, K., Steele, C.J., Löffler, M., Witte, A.V., Schroeter, M.L., Villringer, A., Bazin, P.-L., 2019. Lesion location matters: The relationships between white matter hyperintensities on cognition in the healthy elderly. J. Cereb. blood flow Metab. Off. J. Int. Soc. Cereb. Blood Flow Metab. 39, 36–43. https://doi.org/10.1177/0271678X17740501.

Landau, S.M., Fero, A., Baker, S.L., Koeppe, R., Mintun, M., Chen, K., Reiman, E.M., Jagust, W.J., 2015. Measurement of Longitudinal β-Amyloid Change with ¹⁸F-Florbetapir PET and Standardized Uptake Value Ratios. J. Nucl. Med. 56, 567 LP – 574. 10.2967/jnumed.114.148981.

Landau, S.M., Thomas, B.A., Thurfjell, L., Schmidt, M., Margolin, R., Mintun, M., Pontecorvo, M., Baker, S.L., Jagust, W.J., Initiative, the A.D.N.,, 2014. Amyloid PET imaging in Alzheimer's disease: a comparison of three radiotracers. Eur. J. Nucl. Med. Mol. Imaging 41, 1398–1407. https://doi.org/10.1007/s00259-014-2753-3.

Lane, C.A., Barnes, J., Nicholas, J.M., Sudre, C.H., Cash, D.M., Malone, I.B., Parker, T.D., Keshavan, A., Buchanan, S.M., Keuss, S.E., James, S.-N., Lu, K., Murray-Smith, H., Wong, A., Gordon, E., Coath, W., Modat, M., Thomas, D., Richards, M., Fox, N.C., Schott, J.M., 2020. Associations Between Vascular Risk Across Adulthood and Brain Pathology in Late Life: Evidence From a British Birth Cohort. JAMA Neurol. 77, 175–183. https://doi.org/10.1001/jamaneurol.2019.3774.

Lee, S., Viqar, F., Zimmerman, M.E., Narkhede, A., Tosto, G., Benzinger, T.L.S., Marcus, D.S., Fagan, A.M., Goate, A., Fox, N.C., Cairns, N.J., Holtzman, D.M., Buckles, V., Ghetti, B., McDade, E., Martins, R.N., Saykin, A.J., Masters, C.L., Ringman, J.M., Ryan, N.S., Förster, S., Laske, C., Schofield, P.R., Sperling, R.A., Salloway, S., Correia, S., Jack Jr, C., Weiner, M., Bateman, R.J., Morris, J.C., Mayeux, R., Brickman, A.M., Network, D.I.A., 2016. White matter hyperintensities are a core feature of Alzheimer's disease: Evidence from the dominantly inherited Alzheimer network. Ann. Neurol. 79, 929–939. https://doi.org/10.1002/ana.24647.

Li, X., Liang, Y., Chen, Y., Zhang, J., Wei, D., Chen, K., Shu, N., Reiman, E.M., Zhang, Z., 2015. Disrupted Frontoparietal Network Mediates White Matter Structure Dysfunction Associated with Cognitive Decline in Hypertension Patients. J. Neurosci. 35 (27), 10015–10024.

Liao, D., Cooper, L., Cai, J., Toole, J.F., Bryan, N.R., Hutchinson, R.G., Tyroler, H.A., 1996. Presence and Severity of Cerebral White Matter Lesions and Hypertension, Its Treatment, and Its Control. Stroke 27 (12), 2262–2270.

Liao, D., Cooper, L., Cai, J., Toole, J., Bryan, N., Burke, G., Shahar, E., Nieto, J., Mosley, T., Heiss, G., 1997. The Prevalence and Severity of White Matter Lesions, Their Relationship with Age, Ethnicity, Gender, and Cardiovascular Disease Risk Factors: The ARIC Study. Neuroepidemiology 16, 149–162. https://doi.org/10.1159/000368814.

Lin, J., Wang, D., Lan, L., Fan, Y., 2017. Multiple Factors Involved in the Pathogenesis of White Matter Lesions. Biomed Res. Int. 2017, 9372050. https://doi.org/10.1155/2017/9372050.

Lorius, N., Locascio, J.J., Rentz, D.M., Johnson, K.A., Sperling, R.A., Viswanathan, A., Marshall, G.A., 2015. Vascular disease and risk factors are associated with cognitive decline in the alzheimer disease spectrum. Alzheimer Dis. Assoc. Disord. 29, 18–25. https://doi.org/10.1097/WAD.0000000000000043.

Lowe, V.J., Bruinsma, T.J., Min, H.-K., Lundt, E.S., Fang, P., Senjem, M.L., Boeve, B.F., Josephs, K.A., Pandey, M.K., Murray, M.E., Kantarci, K., Jones, D.T., Schwarz, C.G., Knopman, D.S., Petersen, R.C., Jack Jr., C.R., 2018. Elevated medial temporal lobe and pervasive brain tau-PET signal in normal participants. Alzheimer's Dement. Diagnosis. Assess. Dis. Monit. 10, 210–216. https://doi.org/10.1016/j.dadm.2018.01.005.

Luchsinger, J.A., Reitz, C., Honig, L.S., Tang, M.X., Shea, S., Mayeux, R., 2005. Aggregation of vascular risk factors and risk of incident Alzheimer disease. Neurology 65, 545 LP – 551. 10.1212/01.wnl.0000172914.08967.dc.

Lyall, D.M., Cox, S.R., Lyall, L.M., Celis-Morales, C., Cullen, B., Mackay, D.F., Ward, J., Strawbridge, R.J., McIntosh, A.M., Sattar, N., Smith, D.J., Cavanagh, J., Deary, I.J., Pell, J.P., 2020. Association between APOE e4 and white matter hyperintensity volume, but not total brain volume or white matter integrity. Brain Imaging Behav. 14, 1468–1476. https://doi.org/10.1007/s11682-019-00069-9.

Maillard, P., Carmichael, O.T., Reed, B., Mungas, D., DeCarli, C., 2015. Cooccurrence of vascular risk factors and late-life white-matter integrity changes. Neurobiol. Aging 36, 1670–1677. https://doi.org/10.1016/j.neurobiolaging.2015.01.007.

Merz, A.A., Cheng, S., 2016. Sex differences in cardiovascular ageing. Heart 102, 825 LP – 831. 10.1136/heartjnl-2015-308769.

Morrison, C., Dadar, M., Villeneuve, S., Collins, D.L., 2022. White matter lesions may be an early marker for age-related cognitive decline. NeuroImage. Clin. 35, 103096 https://doi.org/10.1016/j.nicl.2022.103096.

Mortamais, M., Artero, S., Ritchie, K., 2014. White Matter Hyperintensities as Early and Independent Predictors of Alzheimer's Disease Risk. J. Alzheimer's Dis. 42, S393–S400. https://doi.org/10.3233/JAD-141473.

Moscoso, A., Rey-Bretal, D., Silva-Rodríguez, J., Aldrey, J.M., Cortés, J., Pías-Peleteiro, J., Ruibal, Á., Aguiar, P., 2020. White matter hyperintensities are associated with subthreshold amyloid accumulation. Neuroimage 218, 116944. https://doi.org/10.1016/j.neuroimage.2020.116944.

Murray, A.D., Staff, R.T., Shenkin, S.D., Deary, I.J., Starr, J.M., Whalley, L.J., 2005. Brain white matter hyperintensities: relative importance of vascular risk factors in nondemented elderly people. Radiology 237, 251–257. https://doi.org/10.1148/radiol.2371041496.

Palmqvist, S., Zetterberg, H., Mattsson, N., Johansson, P., Minthon, L., Blennow, K., Olsson, M., Hansson, O., 2015. Detailed comparison of amyloid PET and CSF biomarkers for identifying early Alzheimer disease. Neurology 85, 1240–1249. https://doi.org/10.1212/WNL.0000000000001991.

Palmqvist, S., Schöll, M., Strandberg, O., Mattsson, N., Stomrud, E., Zetterberg, H., Blennow, K., Landau, S., Jagust, W., Hansson, O., 2017. Earliest accumulation of β-amyloid occurs within the default-mode network and concurrently affects brain connectivity. Nat. Commun. 8, 1214. https://doi.org/10.1038/s41467-017-01150-x.

Pico, F., Dufouil, C., Lévy, C., Besançon, V., de Kersaint-Gilly, A., Bonithon-Kopp, C., Ducimetière, P., Tzourio, C., Alpérovitch, A., 2002. Longitudinal Study of Carotid Atherosclerosis and White Matter Hyperintensities: The EVA-MRI Cohort. Cerebrovasc. Dis. 14, 109–115. https://doi.org/10.1159/000064741.

Provenzano, F.A., Muraskin, J., Tosto, G., Narkhede, A., Wasserman, B.T., Griffith, E.Y., Guzman, V.A., Meier, I.B., Zimmerman, M.E., Brickman, A.M., Initiative, A.D.N., 2013. White matter hyperintensities and cerebral amyloidosis: necessary and sufficient for clinical expression of Alzheimer disease? JAMA Neurol. 70, 455–461. https://doi.org/10.1001/jamaneurol.2013.1321.

Rabin, J.S., Yang, H.-S., Schultz, A.P., Hanseeuw, B.J., Hedden, T., Viswanathan, A., Gatchel, J.R., Marshall, G.A., Kilpatrick, E., Klein, H., Rao, V., Buckley, R.F., Yau, W.-Y.-W., Kirn, D.R., Rentz, D.M., Johnson, K.A., Sperling, R.A., Chhatwal, J.P., 2019. Vascular Risk and β-Amyloid Are Synergistically Associated with Cortical Tau. Ann. Neurol. 85, 272–279. https://doi.org/10.1002/ana.25399.

Reuter, M., Fischl, B., 2011. Avoiding asymmetry-induced bias in longitudinal image processing. Neuroimage 57, 19–21. https://doi.org/10.1016/j.neuroimage.2011.02.076.

Reuter, M., Rosas, H.D., Fischl, B., 2010. Highly accurate inverse consistent registration: A robust approach. Neuroimage 53, 1181–1196. https://doi.org/10.1016/j.neuroimage.2010.07.020.

Reuter, M., Schmansky, N.J., Rosas, H.D., Fischl, B., 2012. Within-subject template estimation for unbiased longitudinal image analysis. Neuroimage 61, 1402–1418. https://doi.org/10.1016/j.neuroimage.2012.02.084.

Rojas, S., Brugulat-Serrat, A., Bargalló, N., Minguillón, C., Tucholka, A., Falcon, C., Carvalho, A., Morán, S., Esteller, M., Gramunt, N., Fauria, K., Camí, J., Molinuevo, J. L., Gispert, J.D., 2018. Higher prevalence of cerebral white matter hyperintensities in homozygous APOE-ε4 allele carriers aged 45–75: Results from the ALFA study. J. Cereb. Blood Flow Metab. 38, 250–261. https://doi.org/10.1177/0271678X17707397.

Roseborough, A., Ramirez, J., Black, S.E., Edwards, J.D., 2017. Associations between amyloid β and white matter hyperintensities: A systematic review. Alzheimers Dement. 13, 1154–1167. https://doi.org/10.1016/j.jalz.2017.01.026.

Sachdev, P.S., Parslow, R., Wen, W., Anstey, K.J., Easteal, S., 2009. Sex differences in the causes and consequences of white matter hyperintensities. Neurobiol. Aging 30, 946–956. https://doi.org/10.1016/j.neurobiolaging.2007.08.023.

Sardanelli, F., Iozzelli, A., Cotticelli, B., Losacco, C., Cutolo, M., Sulli, A., Nobili, F., Rodriguez, G., 2005. White matter hyperintensities on brain magnetic resonance in systemic sclerosis. Ann. Rheum. Dis. 64, 777 LP – 779. 10.1136/ard.2003.018283.

Schöll, M., Lockhart, S.N., Schonhaut, D.R., O'Neil, J.P., Janabi, M., Ossenkoppele, R., Baker, S.L., Vogel, J.W., Faria, J., Schwimmer, H.D., Rabinovici, G.D., Jagust, W.J., 2016. PET Imaging of Tau Deposition in the Aging Human Brain. Neuron 89, 971–982. https://doi.org/10.1016/j.neuron.2016.01.028.

Schuff, N., Woerner, N., Boreta, L., Kornfield, T., Shaw, L.M., Trojanowski, J.Q., Thompson, P.M., Jack Jr, C.R., Weiner, M.W., Initiative, the A.D.N.,, 2009. MRI of hippocampal volume loss in early Alzheimer's disease in relation to ApoE genotype and biomarkers. Brain 132, 1067–1077. https://doi.org/10.1093/brain/awp007.

Ségonne, F., Dale, A.M., Busa, E., Glessner, M., Salat, D., Hahn, H.K., Fischl, B., 2004. A hybrid approach to the skull stripping problem in MRI. Neuroimage 22, 1060–1075. https://doi.org/10.1016/j.neuroimage.2004.03.032.

Segonne, F., Pacheco, J., Fischl, B., 2007. Geometrically Accurate Topology-Correction of Cortical Surfaces Using Nonseparating Loops. IEEE Trans. Med. Imaging 26, 518–529. https://doi.org/10.1109/TMI.2006.887364.

Sepehrband, F., Barisano, G., Sheikh-Bahaei, N., Cabeen, R.P., Choupan, J., Law, M., Toga, A.W., 2019. Image processing approaches to enhance perivascular space visibility and quantification using MRI. Sci. Rep. 9, 12351. https://doi.org/10.1038/s41598-019-48910-x.

Sepehrband, F., Barisano, G., Sheikh-Bahaei, N., Choupan, J., Cabeen, R.P., Lynch, K.M., Crawford, M.S., Lan, H., Mack, W.J., Chui, H.C., Ringman, J.M., Toga, A.W., 2021. Volumetric distribution of perivascular space in relation to mild cognitive impairment. Neurobiol. Aging 99, 28–43. https://doi.org/10.1016/j.neurobiolaging.2020.12.010.

Sepehrband, F., Barisano, G., Yang, H-J., Choupan, J., Toga, A.W., 2020 "WMH and PVS Mapping from Clinical Data Using Semi-Supervised Multi-Modal Convolutional Neural Network." *Proceeding* of *International Society for Magnetic Resonance in Medicine* (2020).

Sled, J.G., Zijdenbos, A.P., Evans, A.C., 1998. A nonparametric method for automatic correction of intensity nonuniformity in MRI data. IEEE Trans. Med. Imaging 17, 87–97. https://doi.org/10.1109/42.668698.

Söderlund, H., Nilsson, L.-G., Berger, K., Breteler, M.M., Dufouil, C., Fuhrer, R., Giampaoli, S., Hofman, A., Pajak, A., Ridder, M. de, Sans, S., Schmidt, R., Launer, L. J., 2006. Cerebral changes on MRI and cognitive function: The CASCADE study. Neurobiol. Aging 27, 16–23. https://doi.org/10.1016/j.neurobiolaging.2004.12.008.

Sperling, R.A., Laviolette, P.S., O'Keefe, K., O'Brien, J., Rentz, D.M., Pihlajamaki, M., Marshall, G., Hyman, B.T., Selkoe, D.J., Hedden, T., Buckner, R.L., Becker, J.A., Johnson, K.A., 2009. Amyloid deposition is associated with impaired default network function in older persons without dementia. Neuron 63, 178–188. https://doi.org/10.1016/j.neuron.2009.07.003.

Sudre, C.H., Cardoso, M.J., Frost, C., Barnes, J., Barkhof, F., Fox, N., Ourselin, S., 2017. APOE ε4 status is associated with white matter hyperintensities volume accumulation rate independent of AD diagnosis. Neurobiol. Aging 53, 67–75. https://doi.org/10.1016/j.neurobiolaging.2017.01.014.

Svenningsson, A.L., Stomrud, E., Insel, P.S., Mattsson, N., Palmqvist, S., Hansson, O., 2019. β-amyloid pathology and hippocampal atrophy are independently associated with memory function in cognitively healthy elderly. Sci. Rep. 9, 11180. https://doi.org/10.1038/s41598-019-47638-y.

Tan, C.H., Chew, J., Zhang, L., Gulyás, B., Chen, C., 2022. Differential effects of white matter hyperintensities and regional amyloid deposition on regional cortical thickness. Neurobiol. Aging 115, 12–19. https://doi.org/10.1016/j.neurobiolaging.2022.03.013.

Thal, D.R., Rüb, U., Orantes, M., Braak, H., 2002. Phases of Aβ-deposition in the human brain and its relevance for the development of AD. Neurology 58, 1791 LP – 1800. 10.1212/WNL.58.12.1791.

Tosto, G., Zimmerman, M.E., Hamilton, J.L., Carmichael, O.T., Brickman, A.M., 2015. The effect of white matter hyperintensities on neurodegeneration in mild cognitive impairment. Alzheimers Dement. 11, 1510–1519. https://doi.org/10.1016/j.jalz.2015.05.014.

Tustison, N.J., Avants, B.B., Cook, P.A., Zheng, Y., Egan, A., Yushkevich, P.A., Gee, J.C., 2010. N4ITK: improved N3 bias correction. IEEE Trans. Med. Imaging 29, 1310–1320. https://doi.org/10.1109/TMI.2010.2046908.

Vemuri, P., Knopman, D.S., Lesnick, T.G., Przybelski, S.A., Mielke, M.M., Graff-Radford, J., Murray, M.E., Roberts, R.O., Vassilaki, M., Lowe, V.J., Machulda, M.M., Jones, D.T., Petersen, R.C., Jack, C.R.J., 2017. Evaluation of Amyloid Protective Factors and Alzheimer Disease Neurodegeneration Protective Factors in Elderly Individuals. JAMA Neurol. 74, 718–726. https://doi.org/10.1001/jamaneurol.2017.0244.

Villemagne, V.L., Doré, V., Burnham, S.C., Masters, C.L., Rowe, C.C., 2018. Imaging tau and amyloid-β proteinopathies in Alzheimer disease and other conditions. Nat. Rev. Neurol. 14, 225–236. https://doi.org/10.1038/nrneurol.2018.9.

Walsh, P., Sudre, C.H., Fiford, C.M., Ryan, N.S., Lashley, T., Frost, C., Barnes, J., 2020. CSF amyloid is a consistent predictor of white matter hyperintensities across the disease course from aging to Alzheimer's disease. Neurobiol. Aging 91, 5–14. https://doi.org/10.1016/j.neurobiolaging.2020.03.008.

Wang, Y.-L., Chen, W., Cai, W.-J., Hu, H., Xu, W., Wang, Z.-T., Cao, X.-P., Tan, L., Yu, J.-T., 2020. Associations of White Matter Hyperintensities with Cognitive Decline: A

Longitudinal Study. J. Alzheimers. Dis. 73, 759–768. https://doi.org/10.3233/JAD-191005.

Wardlaw, J.M., Smith, E.E., Biessels, G.J., Cordonnier, C., Fazekas, F., Frayne, R., Lindley, R.I., O'Brien, J.T., Barkhof, F., Benavente, O.R., Black, S.E., Brayne, C., Breteler, M., Chabriat, H., Decarli, C., de Leeuw, F.-E., Doubal, F., Duering, M., Fox, N.C., Greenberg, S., Hachinski, V., Kilimann, I., Mok, V., van Oostenbrugge, R., Pantoni, L., Speck, O., Stephan, B.C.M., Teipel, S., Viswanathan, A., Werring, D., Chen, C., Smith, C., van Buchem, M., Norrving, B., Gorelick, P.B., Dichgans, M., 2013. Neuroimaging standards for research into small vessel disease and its contribution to ageing and neurodegeneration. Lancet. Neurol. 12, 822–838. https://doi.org/10.1016/S1474-4422(13)70124-8.

Waters, A.B., Mace, R.A., Sawyer, K.S., Gansler, D.A., 2019. Identifying errors in Freesurfer automated skull stripping and the incremental utility of manual intervention. Brain Imaging Behav 13, 1281–1291. https://doi.org/10.1007/s11682-018-9951-8.

Weaver, N.A., Doeven, T., Barkhof, F., Biesbroek, J.M., Groeneveld, O.N., Kuijf, H.J., Prins, N.D., Scheltens, P., Teunissen, C.E., van der Flier, W.M., Biessels, G.J., 2019. Cerebral amyloid burden is associated with white matter hyperintensity location in specific posterior white matter regions. Neurobiol. Aging 84, 225–234. https://doi.org/10.1016/j.neurobiolaging.2019.08.001.

Weiner, M.W., Veitch, D.P., Aisen, P.S., Beckett, L.A., Cairns, N.J., Green, R.C., Harvey, D., Jack, C.R., Jagust, W., Morris, J.C., Petersen, R.C., Salazar, J., Saykin, A. J., Shaw, L.M., Toga, A.W., Trojanowski, J.Q., 2017. The Alzheimer's Disease Neuroimaging Initiative 3: Continued innovation for clinical trial improvement. Alzheimer's Dement. 13, 561–571. https://doi.org/10.1016/j.jalz.2016.10.006.

Wetter, N.C., Hubbard, E.A., Motl, R.W., Sutton, B.P., 2016. Fully automated open-source lesion mapping of T2-FLAIR images with FSL correlates with clinical disability in MS. Brain Behav. 6, e00440.

Williamson, W., Lewandowski, A.J., Forkert, N.D., Griffanti, L., Okell, T.W., Betts, J., Boardman, H., Siepmann, T., McKean, D., Huckstep, O., Francis, J.M., Neubauer, S., Phellan, R., Jenkinson, M., Doherty, A., Dawes, H., Frangou, E., Malamateniou, C., Foster, C., Leeson, P., 2018. Association of Cardiovascular Risk Factors With MRI Indices of Cerebrovascular Structure and Function and White Matter Hyperintensities in Young Adults. JAMA 320, 665–673. https://doi.org/10.1001/jama.2018.11498.

Wilson, P.W.F., D'Agostino, R.B., Levy, D., Belanger, A.M., Silbershatz, H., Kannel, W.B., 1998. Prediction of Coronary Heart Disease Using Risk Factor Categories. Circulation 97, 1837–1847. https://doi.org/10.1161/01.CIR.97.18.1837.

Wu, B.-S., Zhang, Y.-R., Li, H.-Q., Kuo, K., Chen, S.-D., Dong, Q., Liu, Y., Yu, J.-T., 2021. Cortical structure and the risk for Alzheimer's disease: a bidirectional Mendelian randomization study. Transl. Psychiatry 11, 476. https://doi.org/10.1038/s41398-021-01599-x.

Yoshita, M., Fletcher, E., Harvey, D., Ortega, M., Martinez, O., Mungas, D.M., Reed, B.R., DeCarli, C.S., 2006. Extent and distribution of white matter hyperintensities in normal aging, MCI, and AD. Neurology 67, 2192–2198. https://doi.org/10.1212/01.wnl.0000249119.95747.1f.

Zhu, Y.-C., Chabriat, H., Godin, O., Dufouil, C., Rosand, J., Greenberg, S.M., Smith, E.E., Tzourio, C., Viswanathan, A., 2012. Distribution of white matter hyperintensity in cerebral hemorrhage and healthy aging. J. Neurol. 259, 530–536. https://doi.org/10.1007/s00415-011-6218-3.